Shared genetic pathways contribute to risk of hypertrophic and dilated cardiomyopathies with opposite directions of effect

Tadros, Rafik; Francis, Catherine; Xu, Xiao; Vermeer, Alexa M. C.; Harper, Andrew R.; Huurman, Roy; Bisabu, Ken Kelu; Walsh, Roddy; Hoorntje, Edgar T.; te Rijdt, Wouter P.

Published in:
Nature Genetics

DOI:
10.1038/s41588-020-00762-2

Publication date:
2021

LETTERS
https://doi.org/10.1038/s41588-020-00762-2

nature genetics

Check for updates

Shared genetic pathways contribute to risk of hypertrophic and dilated cardiomyopathies with opposite directions of effect

Rafik Tadros[1,2,47]✉, Catherine Francis[3,4,47], Xiao Xu[5,47], Alexa M. C. Vermeer[2,6,7,47], Andrew R. Harper[8,9], Roy Huurman[10], Ken Kelu Bisabu[1], Roddy Walsh[2], Edgar T. Hoorntje[11,12], Wouter P. te Rijdt[11,12], Rachel J. Buchan[3,4], Hannah G. van Velzen[10], Marjon A. van Slegtenhorst[13], Jentien M. Vermeulen[14], Joost Allard Offerhaus[2], Wenjia Bai[15,16], Antonio de Marvao[5], Najim Lahrouchi[2], Leander Beekman[2], Jacco C. Karper[17], Jan H. Veldink[18], Elham Kayvanpour[19,20], Antonis Pantazis[3], A. John Baksi[4,3], Nicola Whiffin[3,4,5], Francesco Mazzarotto[3,4,21,22], Geraldine Sloane[3,4], Hideaki Suzuki[16,23,24], Deborah Schneider-Luftman[25,26], Paul Elliott[26], Pascale Richard[27,28], Flavie Ader[27,28,29], Eric Villard[28], Peter Lichtner[30], Thomas Meitinger[31,30,32], Michael W. T. Tanck[33], J. Peter van Tintelen[6,34], Andrew Thain[35], David McCarty[35], Robert A. Hegele[35], Jason D. Roberts[35], Julie Amyot[1], Marie-Pierre Dubé[36], Julia Cadrin-Tourigny[1], Geneviève Giraldeau[1], Philippe L. L'Allier[1], Patrick Garceau[1], Jean-Claude Tardif[36], S. Matthijs Boekholdt[37], R. Thomas Lumbers[38,39,40], Folkert W. Asselbergs[41,42], Paul J. R. Barton[3,4], Stuart A. Cook[4,5,43,44], Sanjay K. Prasad[3,4], Declan P. O'Regan[5], Jolanda van der Velden[45], Karin J. H. Verweij[14], Mario Talajic[1], Guillaume Lettre[36], Yigal M. Pinto[2,7], Benjamin Meder[19], Philippe Charron[7,28,46], Rudolf A. de Boer[17], Imke Christiaans[11], Michelle Michels[10], Arthur A. M. Wilde[2,7], Hugh Watkins[8,9,47], Paul M. Matthews[16,47], James S. Ware[3,4,5,47]✉ and Connie R. Bezzina[2,7,47]✉

The heart muscle diseases hypertrophic (HCM) and dilated (DCM) cardiomyopathies are leading causes of sudden death and heart failure in young, otherwise healthy, individuals. We conducted genome-wide association studies and multi-trait analyses in HCM (1,733 cases), DCM (5,521 cases) and nine left ventricular (LV) traits (19,260 UK Biobank participants with structurally normal hearts). We identified 16 loci associated with HCM, 13 with DCM and 23 with LV traits. We show strong genetic correlations between LV traits and cardiomyopathies, with opposing effects in HCM and DCM. Two-sample Mendelian randomization supports a causal association linking increased LV contractility with HCM risk. A polygenic risk score explains a significant portion of phenotypic variability in carriers of HCM-causing rare variants. Our findings thus provide evidence that polygenic risk score may account for variability in Mendelian diseases. More broadly, we provide insights into how genetic pathways may lead to distinct disorders through opposing genetic effects.

Cardiomyopathies are heritable heterogeneous diseases characterized by changes in myocardial structure and function. We sought to better understand the genetic underpinnings of HCM and DCM as well as their relation to myocardial traits in the general population (Fig. 1). HCM has a prevalence of 0.2% (ref. [1]) and has been classically considered a Mendelian disease. However, genetic testing identifies a causal rare variant in less than half of cases[2], and data from both families and population cohorts support reduced penetrance and variable expressivity[3], suggesting a complex genetic architecture. Here, we performed a meta-analysis of three new genome-wide association studies (GWAS) comprising 1,733 unrelated HCM cases and 6,628 controls of European ancestry from the Netherlands, the United Kingdom and Canada (Supplementary Table 1). Of the cases, 642 (37%) carried pathogenic or likely pathogenic variants in established HCM disease genes (Supplementary Table 2). Analysis of SNP-based heritability (h^2_{SNP}) using generalized restricted maximum likelihood (GREML)[4] demonstrated that a significant portion of HCM liability is attributed to common genetic variation (Supplementary Table 3), with h^2_{SNP} estimates in meta-analyses ranging from 0.12 (GREML, fixed-effects; $P=8\times10^{-6}$) to 0.29 (GREML with linkage disequilibrium (LD) and MAF stratification (GREML-LDMS)[5], random effects; $P=9\times10^{-3}$). The GWAS summary meta-analysis results of 6,530,233 variants with a minor allele frequency (MAF) $\geq$ 0.01 are shown as Manhattan and quantile–quantile (QQ) plots in Fig. 2a. The wide association signal observed on chromosome 11 tagging recurrent *MYBPC3* founder variants disappeared when restricting the analysis to the 1,445 HCM cases without such variants (Supplementary

A full list of affiliations appears at the end of the paper.

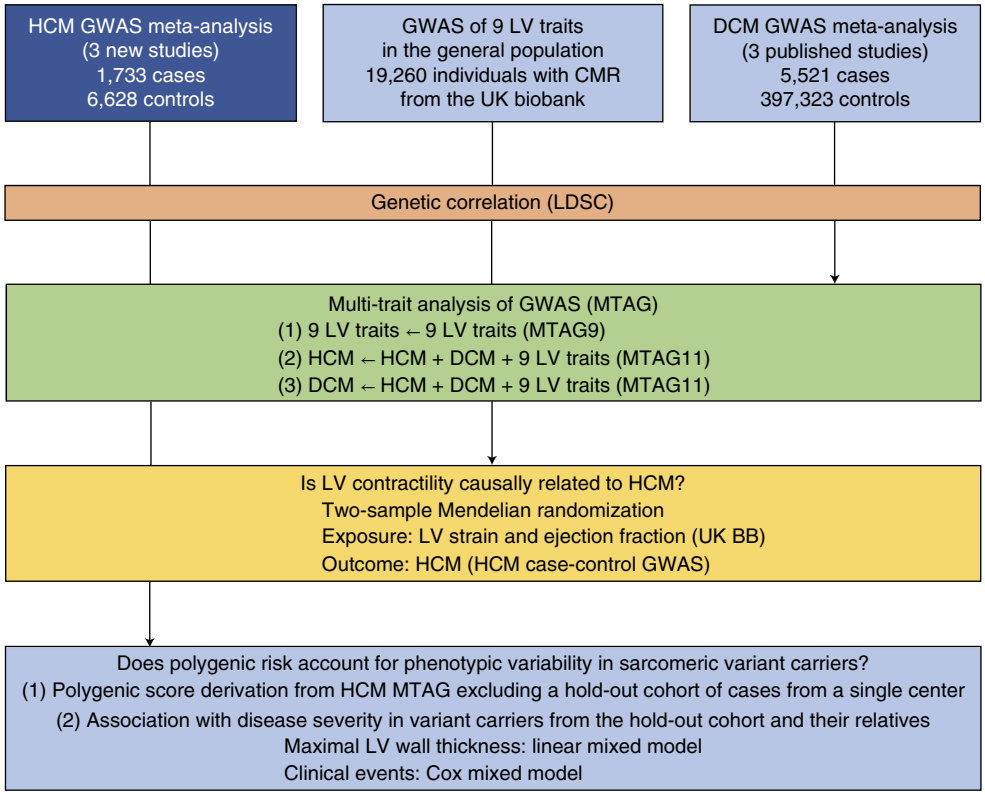

Fig. 1 | Study flowchart. Flowchart of study design.

Fig. 1). Using a conservative threshold of $P < 1 \times 10^{-8}$ to account for multiple testing, a total of six loci were significantly associated with HCM (Table 1, Supplementary Table 4 and Supplementary Fig. 2), of which five are new and one, on chromosome 18 near *FHOD3*, has been previously published[6]. Importantly, two of the new HCM loci (chromosome 1 near *HSPB7* and chromosome 10 near *BAG3*) have been previously associated with DCM at genome-wide statistical significance, but with an opposite direction of effect[7–10]. Specifically, the published DCM lead risk alleles at both loci (rs10927875-C and rs2234962-T)[10] were protective for HCM in the present study (odds ratio, OR (95% confidence interval, CI), 0.80 (0.74–0.87) and 0.71 (0.64–0.77), respectively). Recently, both loci were also found to be associated with LV ejection fraction (LVEF, a volume-based assessment of LV contractility) in the general population[11], for whom DCM risk alleles decrease LVEF (contractility), while HCM risk alleles increase LVEF (contractility). This indicates that genetic loci underlying variability of LV function in the general population may be differentially involved in susceptibility to HCM and DCM.

The observation that two loci with opposite directions of effects in HCM and DCM are also associated with LVEF in the general population motivated us to further explore such relationships between HCM, DCM and LV traits in the general population. We performed a meta-analysis of three published DCM case–control genetic association studies[7–9] totaling 5,521 cases and 397,323 controls (Supplementary Table 5), as well as GWAS of nine LV traits derived from cardiac magnetic resonance (CMR) imaging in a cohort of 19,260 participants in UK Biobank (UKBB) without structural heart disease (Supplementary Table 6 and Supplementary Figs. 3–5). Compared to published GWAS on LV traits[11], our analysis adds new phenotypes including mean LV wall thickness (meanWT) and measures of myocardial deformation (that is, strain), which are proposed as more direct markers of contractility than volumetric assessments (LVEF)[12]. Many LV trait pairs were correlated phenotypically (Supplementary Fig. 6). The Manhattan and QQ plots of the DCM meta-analysis and nine LV traits GWAS are presented in panels **a** of Extended Data Figs. 1–10. A total of three loci in the DCM (all previously published[7,8]; Supplementary Table 7 and Supplementary Fig. 7) and 17 loci in any of the nine LV traits meta-analyses reached a *P*-value threshold of 1×10^{-8} (Supplementary Table 8).

Genetic correlations between LV traits in the general population, HCM and DCM were assessed using LD score regression[13,14] (Supplementary Table 9). The results highlight the divergent relationships of LV traits with DCM and HCM (Fig. 3). HCM showed a positive genetic correlation with meanWT ($r_g = 0.51$, $P = 9 \times 10^{-6}$), while DCM was positively correlated with LV end-diastolic (LVEDV) and end-systolic (LVESV) volumes ($r_g = 0.43$, $P = 2 \times 10^{-4}$ and $r_g = 0.46$, $P = 1 \times 10^{-4}$, respectively). Decreased LV contractility is a hallmark of DCM, and we observed a negative genetic correlation between DCM and LV contractility, whether assessed using a volumetric measure, LVEF ($r_g = -0.35$, $P = 9 \times 10^{-3}$), or using global LV strain measured in any direction: circumferential (-strain^{circ}; $r_g = -0.48$, $P = 2 \times 10^{-4}$), radial (strain^{rad}; $r_g = -0.42$, $P = 3 \times 10^{-3}$) and longitudinal (-strain^{long}; $r_g = -0.27$, $P = 0.05$) (note that for strain^{long} and strain^{circ}, increasingly negative values reflect higher strain/contractility). Remarkably, all four of these contractility parameters were positively correlated with HCM; increases in contractility are correlated with increased HCM risk (r_g ranging from 0.27 for -strain^{long} ($P = 0.03$) to 0.62 for -strain^{circ} ($P = 1 \times 10^{-7}$)).

We then performed multi-trait analysis of GWAS (MTAG)[15] to increase power for discovery of novel loci. Two analyses were performed: (1) MTAG of nine LV traits (referred to as MTAG9) to uncover novel loci associated with LV traits and (2) MTAG of HCM, DCM and nine LV traits (henceforth MTAG11) to uncover loci associated with DCM and HCM. The corresponding Manhattan and QQ plots appear as panels **b** in Fig. 2 and Extended Data Figs. 1–10. MTAG9 uncovered six additional genetic loci associated with LV traits (Supplementary Table 8). MTAG11 uncovered an additional

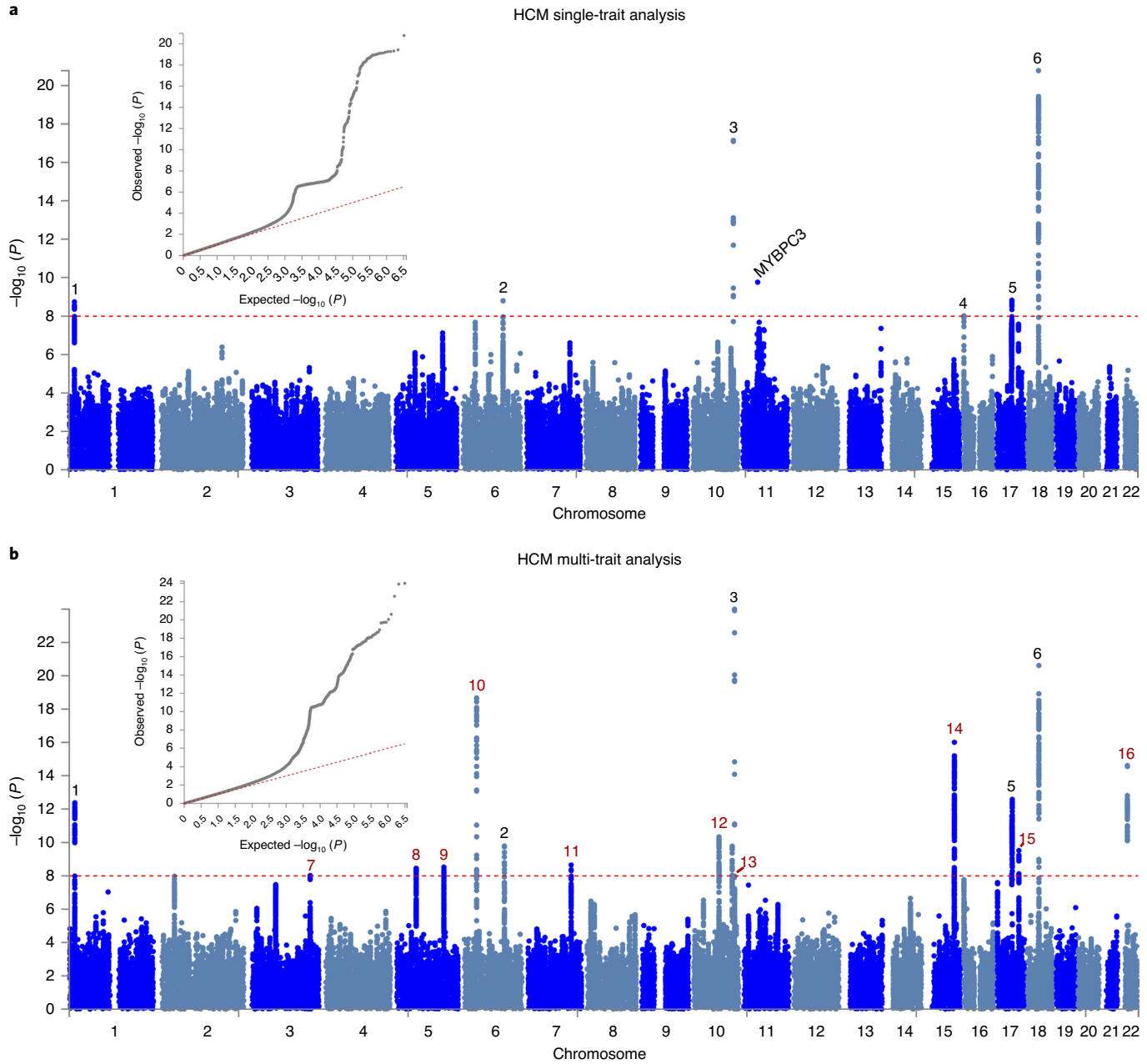

Fig. 2 | Summary results of HCM single-trait GWAS and multi-trait analysis. a,b, Single-trait analysis (**a**) consisted of a fixed-effects meta-analysis of case–control GWAS using a frequentist test, and multi-trait analysis results (**b**) were obtained using MTAG for HCM, including GWAS for DCM and nine LV traits. Summary statistics shown as Manhattan plots with red dashed line showing the genome-wide significance threshold of $P=1\times10^{-8}$. QQ plots are shown as inserts in corresponding panels. Genomic inflation (λ) = 1.081 (single-trait) and 1.082 (MTAG). Six association signals were identified in single-trait analysis (**a**) and an additional 10 signals were identified in multi-trait analysis (**b**). The wide signal on chromosome 11 tags founder *MYBPC3* pathogenic variants. Locus no. 4 was only significant in the single-trait analysis and did not replicate in an independent HCM GWAS. Numbering of signals is as shown in Table 1 and Supplementary Table 4, where red numbers refer to signals reaching genome-wide significance only in the multi-trait analysis.

10 HCM (Table 1, Supplementary Table 4 and Supplementary Fig. 2) and 10 DCM loci (Supplementary Table 7 and Supplementary Fig. 7). Supplementary Tables 4, 7 and 8 tabulate relationships for all traits with all HCM, DCM and LV trait lead SNPs, respectively, highlighting the cross-trait single SNP level correlation. In particular, 8 of the 16 HCM-associated loci also showed significant association with DCM using a Benjamin–Hochberg false discovery rate (FDR) < 0.05, where all 8 lead SNPs showed opposite directions of effect in HCM versus DCM (Supplementary Table 4). Similarly, all 13 DCM loci were also associated with HCM at an FDR < 0.05 (Supplementary Table 7), with all loci showing an opposite effect in HCM versus DCM except locus DCM4 near *TTN*. At this locus, the DCM risk allele also increases risk for HCM. We hypothesize that this unique concordant HCM/DCM effect may be attributable to pleiotropic effects of that locus on LV structure/function, where the HCM and DCM risk increasing allele reduces LV contractility parameters but also increases LV hypertrophy (LV mass and meanWT; Supplementary Table 7). Figure 4 displays a heatmap representation of the direction and strength of effect of all 16 HCM risk alleles and 13 DCM risk alleles in all nine LV traits, HCM and

Table 1 | Lead SNPs and effect estimates for genome-wide significant loci ($P<1\times10^{-8}$) in the HCM single-trait and multi-trait analyses

Locus	Lead SNP	GRCh37	Nearest gene	RA	NRA	RAF	OR	95% CI	*P*	*P* (MTAG11)	$P_{replication}$
HCM1	rs10927886	1:16339313	*HSPB7*	G	C	0.41	1.28	1.18–1.38	1.8×10^{-9}	7.4×10^{-13}	2.5×10^{-13}
HCM2	rs12212795	6:118654308	*SLC35F1*	C	G	0.06	1.69	1.43–2.01	1.6×10^{-9}	1.7×10^{-10}	6.7×10^{-11}
HCM3	rs17099139	10:121419487	*BAG3*	G	C	0.29	1.46	1.34–1.59	7.2×10^{-18}	1.0×10^{-24}	1.3×10^{-22}
HCM4[a]	rs9928278	16:2152651	*PKD1*	C	T	0.18	1.45	1.28–1.65	9.5×10^{-9}	5.9×10^{-7}	2.7×10^{-1}
HCM5	rs1378358	17:44787312	*NSF*	T	C	0.23	1.34	1.22–1.47	1.5×10^{-9}	4.7×10^{-13}	4.7×10^{-8}
HCM6	rs503274	18:34253745	*FHOD3*	C	T	0.31	1.52	1.40–1.66	1.7×10^{-21}	2.4×10^{-21}	4.3×10^{-19}
HCM7 (MTAG11)	rs9647379	3:171785168	*FNDC3B*	C	G	0.42	1.22	1.12–1.33	6.8×10^{-6}	9.5×10^{-9}	2.4×10^{-6}
HCM8 (MTAG11)	rs2191445	5:57011469	*ACTBL2*	T	A	0.78	1.29	1.17–1.43	8.0×10^{-7}	3.5×10^{-9}	2.6×10^{-5}
HCM9 (MTAG11)	rs4385202	5:138743256	*DNAJC18*	A	G	0.31	1.25	1.15–1.37	6.0×10^{-7}	3.0×10^{-9}	7.3×10^{-5}
HCM10 (MTAG11)	rs66761782	6:36636080	*CDKN1A*	C	T	0.26	1.29	1.18–1.41	3.4×10^{-8}	2.1×10^{-19}	1.3×10^{-8}
HCM11 (MTAG11)	rs60871386	7:128430437	*CCDC136*	T	G	0.10	1.43	1.25–1.64	3.4×10^{-7}	2.2×10^{-9}	1.4×10^{-4}
HCM12 (MTAG11)	rs3740293	10:75406141	*SYNPO2L*	C	A	0.15	1.33	1.19–1.49	4.8×10^{-7}	4.6×10^{-11}	8.5×10^{-6}
HCM13 (MTAG11)	rs11196078	10:114487812	*VTI1A*	A	G	0.26	1.26	1.15–1.38	5.2×10^{-7}	1.6×10^{-10}	6.7×10^{-7}
HCM14 (MTAG11)	rs11073729	15:85350081	*ZNF592*	C	T	0.46	1.20	1.11–1.30	4.2×10^{-6}	9.9×10^{-17}	3.6×10^{-7}
HCM15 (MTAG11)	rs9892651	17:64303793	*PRKCA*	T	C	0.59	1.25	1.16–1.36	2.8×10^{-8}	3.0×10^{-10}	2.4×10^{-9}
HCM16 (MTAG11)	rs2186370	22:24171305	*SMARCB1*	A	G	0.22	1.21	1.09–1.34	3.5×10^{-4}	2.5×10^{-15}	5.5×10^{-15}

[a]Locus HCM4 is not replicated. GRCh37, genomic position in GRCh37; MTAG11, multi-trait analysis of GWAS summary statistics from HCM, DCM and nine quantitative LV traits; NRA, nonrisk allele; OR, odds ratio for each risk allele in the single-trait HCM analysis; *P*, single-trait analysis *P* value; *P* (MTAG11), multi-trait analysis *P* value for HCM; $P_{replication}$, *P* value in the replication dataset; RA, risk allele; RAF, risk allele frequency.

DCM. Many HCM risk alleles are also associated with reduced risk of DCM and, in the general population, increased LV contractility (LVEF and strain) and decreased LV volumes.

Replication of HCM loci was tested in an independent dataset[16] comprising 2,694 HCM cases included from the Hypertrophic Cardiomyopathy Registry (HCMR)[17] or the National Institute for Health Research (NIHR) Bioresource for Rare Disease (BRRD)[18], and 47,486 controls without HCM included from the UKBB or BRRD. Of the 16 HCM loci, 15 (all except HCM4) were replicated at $P<0.003$ (Table 1 and Supplementary Table 10).

The correlation between increased contractility and HCM risk led us to test the hypothesis that increased contractility is causally associated with HCM. We tested such potential causality between increased LV contractility and HCM using two-sample Mendelian randomization (MR), where the exposure variables were LV contractility measures (-strain^{circ}, strain^{rad}, -strain^{long} and LVEF; all strongly correlated, with overlap in associated loci) and the outcome was HCM. Genetic instruments for the exposures were selected using two approaches: (1) independent SNPs reaching $P<5\times10^{-8}$ in the single-trait analysis and (2) those reaching $P<5\times10^{-8}$ in MTAG9 analysis (Supplementary Table 11). The results of the primary inverse-variance weighted (IVW) analysis and sensitivity analyses including leave-one-out analyses are presented in Supplementary Table 12 and Supplementary Figs. 8 and 9. Although heterogeneity and the limited number of SNPs in the exposure–outcome effects are limitations, the findings of the main (IVW) and sensitivity analyses support a causal relation between increased LV contractility and increased HCM risk. Both SNP selection approaches demonstrate a significant effect of -strain^{circ} on the odds of HCM (OR 1.89 (1.32–2.70), $P=5\times10^{-4}$ and OR 1.94 (1.43–2.63), $P=2\times10^{-5}$, for approaches (1) and (2), respectively), while the effect of strain^{rad} and LVEF on HCM risk was significant only using the latter more SNP inclusive approach (2) in the IVW model (OR 1.38 (1.18–1.62), $P=8\times10^{-5}$ and OR 1.37 (1.10–1.69), $P=4\times10^{-3}$, for strain^{rad} and LVEF, respectively). The effect of strain^{long} on HCM was not significant. Notably, the magnitude of HCM risk increase with increased contractility is important; for example, each unit (1%) increase in LVEF and -strain^{circ} increases the risk of HCM by 37% and 89%, respectively (Supplementary Table 12). To place this in context, the standard deviations of LVEF and strain^{circ} in the UKBB are 5.5% and 3.1%, respectively.

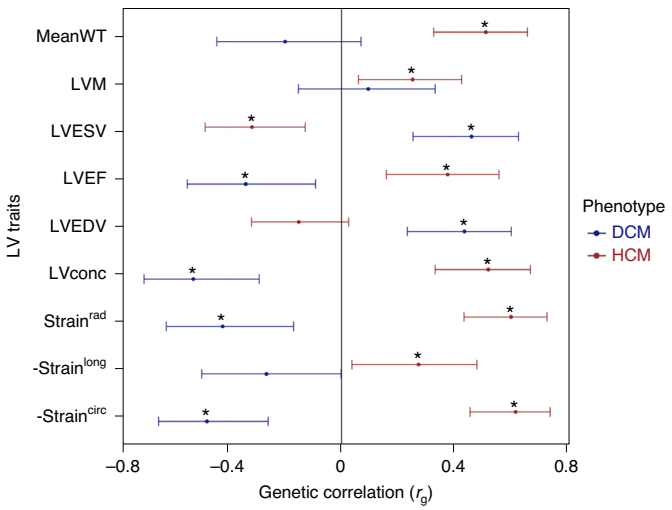

Fig. 3 | Genetic correlation between LV traits, HCM and DCM. HCM (red bars) and DCM (blue bars) show strong genetic correlations with quantitative cardiac LV traits measured in the general population, but with opposite effects. Center values are the estimated genetic correlation (r_g) and error bars indicate 95% CI. Samples sizes for included GWAS are as follows: 1,733 cases and 6,628 controls for HCM; 5,521 cases and 397,323 controls for DCM and 19,260 for LV traits. Asterisks identify significant genetic correlations with a Benjamini–Hochberg FDR < 0.05. Data shown correspond to that in Supplementary Table 9. Since strain^{circ} and strain^{long} are always negative values, -strain^{circ} and -strain^{long} are plotted to facilitate interpretation of effect direction.

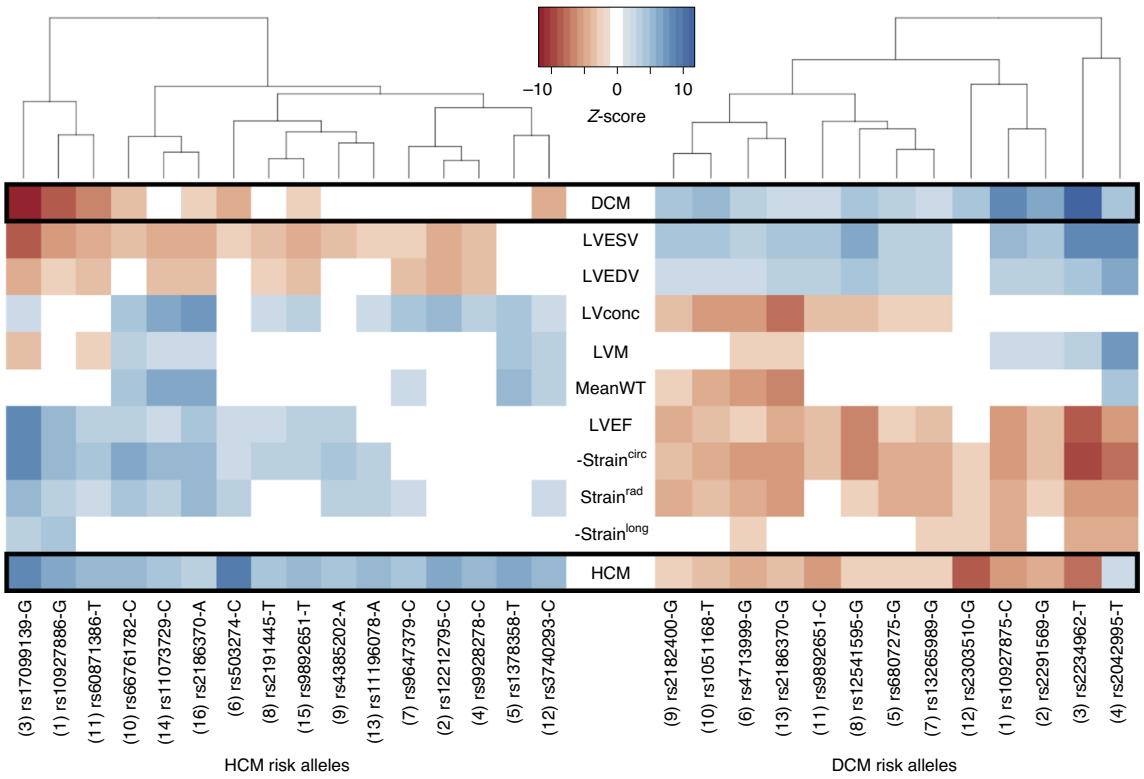

Fig. 4 | Cross-trait associations of HCM and DCM loci. Heatmap of cross-trait associations of the 16 HCM (left side) and 13 DCM (right) risk variants in HCM, DCM and nine LV traits in the general population. The dbSNP ID and risk alleles are shown on the *x*-axis, with the corresponding locus number in parenthesis (corresponding to numbering in Fig. 2, Table 1 and Supplementary Table 4 for HCM, and Extended Data Fig. 1 and Supplementary Table 7 for DCM). Variants sorted along the *x*-axis using Euclidean distance and complete hierarchical clustering (dendrogram on top). Effect of the HCM or DCM risk alleles shown as a colormap of *Z*-scores (legend), where positive values (concordant effect) are in shades of blue and negative values (discordant effect) are in shades of red. Only associations with FDR < 0.05 are shown. HCM and DCM loci show many and reciprocal cross-trait associations. Since $\text{strain}^{\text{circ}}$ and $\text{strain}^{\text{long}}$ are negative values, we show $\text{-strain}^{\text{circ}}$ and $\text{-strain}^{\text{long}}$ to facilitate interpretation of effect direction. Lookup in DCM was performed using SNP proxies to maximize sample size, as shown in Supplementary Table 4. Note that the DCM risk allele rs2042995-T also increases risk of HCM, potentially through pleiotropic effects (decreased contractility and increased LV wall thickness).

We performed MAGMA[19] gene-based analyses using the HCM and DCM MTAG11 summary statistics. Not surprisingly, gene property analysis for tissue specificity identified muscle (heart and skeletal) as significantly associated with both HCM and DCM (Supplementary Fig. 10). Similarly, MAGMA gene-set analysis identified significantly associated gene sets related to muscle contraction for cellular components (for example, I Band, contractile fiber), biological processes (for example, myofibril assembly and sarcomere organization) and molecular functions (actin binding) (Supplementary Tables 13 and 14). Individual HCM, DCM and LV traits loci were annotated with proxy coding variants, significant expression (eQTL) and splice (sQTL) quantitative trait loci (QTL) in skeletal and heart muscle, and chromatin interactions using Hi-C data obtained in LV tissue (Supplementary Tables 15–18). The established Mendelian cardiomyopathy genes *BAG3* (in loci HCM3, DCM3 and LV10), *ALPK3* (HCM14, DCM10 and LV13), *FHOD3* (HCM6 and DCM12), *TTN* (DCM4 and LV4), *FLNC* (HCM11 and DCM2) and *PLN* (HCM2 and LV8), which directly overlap associated loci (defined with $r^2 > 0.6$ from the lead SNP), are highly plausible candidates for the functional effects of variation at the corresponding loci. The involvement of *FHOD3* and *FLNC* is further supported by eQTL effects, and involvement of *PLN*, *ALPK3* and *TTN* is supported by evidence for Hi-C chromatin interactions between the association loci and the gene promoter. Notably, two loci overlap genes that play key roles in cardiomyocyte calcium handling related with muscle contraction (*PLN* and *CASQ2*; each supported by eQTL effects). Other candidate genes that emerge based on annotation and prior knowledge include *GATA4* (DCM7 and LV19)[20], *PRKCA* (HCM15 and DCM11)[21], *HSPB7* (HCM1, DCM1 and LV1)[22] and *TMEM43* (DCM5)[23]. In aggregate, candidate genes at associated loci suggest susceptibility mechanisms involving regulation of sarcomere assembly, homeostasis and calcium handling in cardiomyocytes.

HCM attributed to rare disease-causing sarcomeric variants is characterized by variable disease severity. We investigated whether common variants could explain such phenotypic variability. We first derived a polygenic risk score (PRS_{HCM}; Supplementary Table 19) from an HCM GWAS meta-analysis excluding a hold-out cohort of cases with sarcomeric variants from a single (Dutch) center. We then assessed the association of PRS_{HCM} with HCM expression and severity in the hold-out cohort and their family members (368 carriers of pathogenic or likely pathogenic sarcomeric variants, Supplementary Table 20). The results are shown in Supplementary Table 21. PRS_{HCM} was associated with maximal LV wall thickness (maxLVWT) indexed to body surface area (BSA), where each standard deviation (SD) increase in the PRS_{HCM} is associated with a $0.7\,\text{mm}\,\text{m}^{-2}$ increase in maxLVWT ($P = 1 \times 10^{-4}$), corresponding to a clinically relevant 1.4 mm absolute increase in maxLVWT for an average BSA of $1.95\,\text{m}^2$ (cohort mean, Dutch population). PRS_{HCM} was also associated with adverse clinical events (a composite of septal reduction therapy, cardiac transplantation, sustained ventricular arrhythmia, sudden cardiac death, appropriate defibrillator therapy

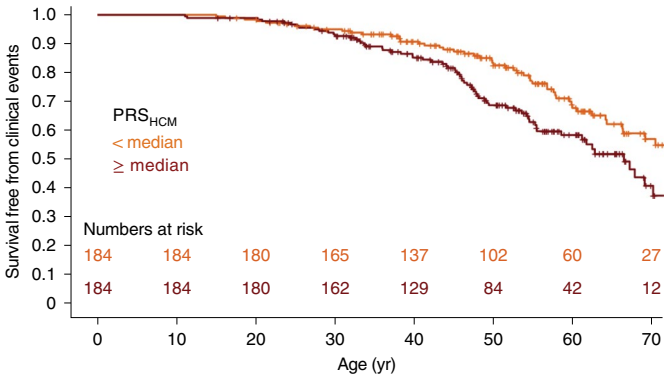

Fig. 5 | A PRS for HCM stratifies event-free survival in carriers of disease-causing variants in sarcomere-encoding genes. Kaplan–Meier curves showing survival free from adverse clinical events (composite of septal reduction therapy, cardiac transplantation, sustained ventricular arrhythmia, sudden cardiac death, appropriate implantable cardioverter defibrillator (ICD) therapy or atrial fibrillation/flutter) in sarcomeric (likely) pathogenic variant carriers stratified by polygenic score (PRS_{HCM}) below (dark orange) versus above (dark red) the median. Numbers at risk in each group along the time scale shown at the bottom of the plot. Ticks along the survival curves represent participant censoring. Two-sided log-rank test $P=0.032$ (Cox proportional hazard analysis $P=9\times10^{-3}$; see Supplementary Table 21).

or atrial fibrillation/flutter), where each SD increase in PRS_{HCM} was associated with a 28% relative risk increase in adverse clinical events (hazard ratio 1.28, 95% CI 1.06–1.54; $P=9\times10^{-3}$). Figure 5 shows the event-free survival in sarcomeric variant carriers stratified by PRS_{HCM} above versus below the median.

Several new observations emerge from this work: (1) by conducting the first well-powered GWAS in HCM and the largest GWAS meta-analysis in DCM, we identified 15 novel loci associated with HCM, of which 14 replicate in an independent cohort, and 7 novel loci for DCM, bringing the total number of loci to 16 and 13, respectively; (2) we identified a total of 23 loci for LV traits and extended the study of these traits to include LV strain (13 loci) and LV wall thickness (6 loci); (3) we demonstrate for the first time a direct genetic correlation between LV traits and susceptibility to HCM and DCM with opposing direction of effect, indicating shared pathways for these disorders; (4) by using MR, we demonstrate that increased cardiac contractility plays an etiologic role in HCM. The demonstration of causal common variant effects on HCM through increased contractility broadens the applicability of therapeutic strategies targeting contractility as has been proposed for rare variants in sarcomere genes[24]; and (5) we provide the first evidence that a polygenic score based on common HCM susceptibility variants may explain interindividual differences in HCM disease severity among carriers of rare disease-causing variants. This work constitutes a proof of principle for potential use of PRS in HCM risk stratification, to be assessed in future purposely designed and adequately powered studies. More broadly, this work demonstrates that the same genetic pathways may lead to distinct disorders through opposing genetic effects.

Online content

Any methods, additional references, Nature Research reporting summaries, source data, extended data, supplementary information, acknowledgements, peer review information; details of author contributions and competing interests; and statements of data and code availability are available at https://doi.org/10.1038/s41588-020-00762-2.

Received: 28 February 2020; Accepted: 10 December 2020;
Published online: 25 January 2021

References

1. Semsarian, C., Ingles, J., Maron, M. S. & Maron, B. J. New perspectives on the prevalence of hypertrophic cardiomyopathy. *J. Am. Coll. Cardiol.* **65**, 1249–1254 (2015).
2. Walsh, R. et al. Quantitative approaches to variant classification increase the yield and precision of genetic testing in Mendelian diseases: the case of hypertrophic cardiomyopathy. *Genome Med.* **11**, 5 (2019).
3. Elliott, P. M. et al. 2014 ESC Guidelines on diagnosis and management of hypertrophic cardiomyopathy: the Task Force for the Diagnosis and Management of Hypertrophic Cardiomyopathy of the European Society of Cardiology (ESC). *Eur. Heart J.* **35**, 2733–2779 (2014).
4. Yang, J. et al. Common SNPs explain a large proportion of the heritability for human height. *Nat. Genet.* **42**, 565–569 (2010).
5. Yang, J. et al. Genetic variance estimation with imputed variants finds negligible missing heritability for human height and body mass index. *Nat. Genet.* **47**, 1114–1120 (2015).
6. Wooten, E. C. et al. Formin homology 2 domain containing 3 variants associated with hypertrophic cardiomyopathy. *Circ. Cardiovasc. Genet.* **6**, 10–18 (2013).
7. Aragam, K. G. et al. Phenotypic refinement of heart failure in a national biobank facilitates genetic discovery. *Circulation* **139**, 489–501 (2019).
8. Esslinger, U. et al. Exome-wide association study reveals novel susceptibility genes to sporadic dilated cardiomyopathy. *PLoS One* **12**, e0172995 (2017).
9. Meder, B. et al. A genome-wide association study identifies 6p21 as novel risk locus for dilated cardiomyopathy. *Eur. Heart J.* **35**, 1069–1077 (2014).
10. Villard, E. et al. A genome-wide association study identifies two loci associated with heart failure due to dilated cardiomyopathy. *Eur. Heart J.* **32**, 1065–1076 (2011).
11. Aung, N. et al. Genome-wide analysis of left ventricular image-derived phenotypes identifies fourteen loci associated with cardiac morphogenesis and heart failure development. *Circulation* **140**, 1318–1330 (2019).
12. Stokke, T. M. et al. Geometry as a confounder when assessing ventricular systolic function: comparison between ejection fraction and strain. *J. Am. Coll. Cardiol.* **70**, 942–954 (2017).
13. Bulik-Sullivan, B. et al. An atlas of genetic correlations across human diseases and traits. *Nat. Genet.* **47**, 1236–1241 (2015).
14. Bulik-Sullivan, B. K. et al. LD Score regression distinguishes confounding from polygenicity in genome-wide association studies. *Nat. Genet.* **47**, 291–295 (2015).
15. Turley, P. et al. Multi-trait analysis of genome-wide association summary statistics using MTAG. *Nat. Genet.* **50**, 229–237 (2018).
16. Harper, A. R. et al. Common genetic variants and modifiable risk factors underpin susceptibility and expressivity in hypertrophic cardiomyopathy. *Nat. Genet.* https://doi.org/10.1038/s41588-020-00764-0 (2021).
17. Kramer, C. M. et al. Hypertrophic Cardiomyopathy Registry: The rationale and design of an international, observational study of hypertrophic cardiomyopathy. *Am. Heart J.* **170**, 223–230 (2015).
18. Turro, E. et al. Whole-genome sequencing of patients with rare diseases in a national health system. *Nature* **583**, 96–102 (2020).
19. de Leeuw, C. A., Mooij, J. M., Heskes, T. & Posthuma, D. MAGMA: generalized gene-set analysis of GWAS data. *PLoS Comput. Biol.* **11**, e1004219 (2015).
20. Oka, T. et al. Cardiac-specific deletion of Gata4 reveals its requirement for hypertrophy, compensation, and myocyte viability. *Circ. Res.* **98**, 837–845 (2006).
21. Braz, J. C. et al. PKC-alpha regulates cardiac contractility and propensity toward heart failure. *Nat. Med.* **10**, 248–254 (2004).
22. Wu, T. et al. HSPB7 is indispensable for heart development by modulating actin filament assembly. *Proc. Natl Acad. Sci. USA* **114**, 11956–11961 (2017).
23. Merner, N. D. et al. Arrhythmogenic right ventricular cardiomyopathy type 5 is a fully penetrant, lethal arrhythmic disorder caused by a missense mutation in the *TMEM43* gene. *Am. J. Hum. Genet.* **82**, 809–821 (2008).
24. Green, E. M. et al. A small-molecule inhibitor of sarcomere contractility suppresses hypertrophic cardiomyopathy in mice. *Science* **351**, 617–621 (2016).

[1]Cardiovascular Genetics Center, Montreal Heart Institute, Faculty of Medicine, Université de Montréal, Montreal, Québec, Canada. [2]Department of Clinical and Experimental Cardiology, Heart Center, Amsterdam Cardiovascular Sciences, University of Amsterdam, Amsterdam UMC, Amsterdam, the Netherlands. [3]Cardiovascular Research Centre, Royal Brompton and Harefield National Health Service Foundation Trust, London, UK. [4]National Heart and Lung Institute, Imperial College London, London, UK. [5]MRC London Institute of Medical Sciences, Imperial College London, London, UK. [6]Department of Clinical Genetics, University of Amsterdam, Amsterdam UMC, Amsterdam, the Netherlands. [7]European Reference Network for Rare and Low Prevalence Complex Diseases of the Heart (ERN GUARD-HEART). [8]Division of Cardiovascular Medicine, Radcliffe Department of Medicine, University of Oxford, Oxford, UK. [9]Wellcome Centre for Human Genetics, Oxford, UK. [10]Department of Cardiology, Thoraxcenter, Erasmus University Medical Center, Rotterdam, the Netherlands. [11]Department of Genetics, University of Groningen, University Medical Center Groningen, Groningen, the Netherlands. [12]Netherlands Heart Institute, Utrecht, the Netherlands. [13]Department of Clinical Genetics, Thoraxcenter, Erasmus University Medical Center, Rotterdam, the Netherlands. [14]Department of Psychiatry, University of Amsterdam, Amsterdam UMC, Amsterdam, the Netherlands. [15]Data Science Institute, Imperial College London, London, UK. [16]Department of Brain Sciences and UK Dementia Research Institute at Imperial College London, Hammersmith Hospital, Imperial College London, London, UK. [17]Department of Cardiology, University of Groningen, University Medical Center Groningen, Groningen, the Netherlands. [18]Department of Neurology, UMC Utrecht Brain Center, University Medical Center Utrecht, Utrecht University, Utrecht, the Netherlands. [19]Institute for Cardiomyopathies, Heidelberg Heart Center, University of Heidelberg, Heidelberg, Germany. [20]DZHK (German Center for Cardiovascular Research), Berlin, Germany. [21]Department of Experimental and Clinical Medicine, University of Florence, Florence, Italy. [22]Cardiomyopathy Unit, Careggi University Hospital, Florence, Italy. [23]Department of Cardiovascular Medicine, Tohoku University Hospital, Seiryo, Aoba, Sendai, Japan. [24]Tohoku Medical Megabank Organization, Tohoku University, Seiryo, Aoba, Sendai, Japan. [25]The Francis Crick Institute, London, UK. [26]Department of Epidemiology and Biostatistics, Imperial College London, London, UK. [27]Service de biochimie métabolique, UF de cardiogénétique et myogénétique moléculaire et cellulaire, APHP, Hôpital Pitié-Salpêtrière, Paris, France. [28]INSERM, UMR_S 1166 and ICAN Institute for Cardiometabolism and Nutrition, Faculté de Médecine, Sorbonne Université, Paris, France. [29]Faculté de Pharmacie, Université de Paris, Paris, France. [30]Institute of Human Genetics, Helmholtz Zentrum Muenchen, Neuherberg, Germany. [31]Klinikum rechts der Isar der TU Muenchen School of Medicine, Institute of Human Genetics, Munich, Germany. [32]DZHK (German Center for Cardiovascular Research), partner site Munich Heart Alliance, Munich, Germany. [33]Department of Clinical Epidemiology, Biostatistics and Bioinformatics, University of Amsterdam, Amsterdam Public Health (APH), Amsterdam UMC, Amsterdam, the Netherlands. [34]Department of Genetics, University Medical Center Utrecht, Utrecht University, Utrecht, the Netherlands. [35]Department of Medicine and Robarts Research Institute, Schulich School of Medicine and Dentistry, Western University, London, Ontario, Canada. [36]Montreal Heart Institute Research Center, Faculty of Medicine, Université de Montréal, Montreal, Québec, Canada. [37]Department of Cardiology, University of Amsterdam, Heartcenter, Amsterdam UMC, Amsterdam, the Netherlands. [38]Institute of Health Informatics, University College London, London, UK. [39]Health Data Research UK, Gibbs Building, London, UK. [40]Barts Heart Centre, Saint Bartholomew's Hospital, London, UK. [41]Department of Cardiology, Division Heart and Lungs, University Medical Center Utrecht, Utrecht University, Utrecht, the Netherlands. [42]Institute of Cardiovascular Science and Institute of Health Informatics, Faculty of Population Health Sciences, University College London, London, UK. [43]National Heart Research Institute Singapore, National Heart Center Singapore, Singapore, Singapore. [44]Cardiovascular and Metabolic Disorders Program, Duke-National University of Singapore Medical School, Singapore, Singapore. [45]Department of Physiology, Amsterdam Cardiovascular Sciences, Amsterdam UMC, Amsterdam, the Netherlands. [46]Département de Génétique, Centre de référence des maladies cardiaques héréditaires ou rares, APHP, Hôpital Pitié-Salpêtrière, Paris, France. [47]These authors contributed equally: Rafik Tadros, Catherine Francis, Xiao Xu, Alexa M. C. Vermeer, Hugh Watkins, Paul M. Matthews, James S. Ware, Connie R. Bezzina. ✉e-mail: rafik.tadros@umontreal.ca; j.ware@imperial.ac.uk; c.r.bezzina@amsterdamumc.nl

Methods

The overall study design and flowchart are shown in Fig. 1 and described in detail below and in the Supplementary Note. All human participants provided written informed consent, and all studies had received approval from the appropriate ethical review boards (see Reporting Summary).

GWAS of HCM. *Case inclusion.* Unrelated people with HCM were included from cardiovascular genetics referral centers (Supplementary Table 1). Cases were included if they had a clinical diagnosis of HCM according to current diagnostic criteria[3]: maxLVWT of ≥15 mm, ≥13 mm in presence of family history of HCM, or *Z*-score > 2 in children, where LV hypertrophy is not solely explained by loading conditions. Cases were excluded if they had syndromic HCM (for example, Noonan syndrome spectrum), metabolic disease (for example Fabry) or had >1 sarcomeric pathogenic or likely pathogenic variants (homozygous, compound heterozygous or digenic). The maxLVWT was collected from chart review of cases using the most recent cardiac imaging report available, before septal reduction therapy or cardiac transplantation, if performed. Because cases were referred from multiple centers for cardiogenetic evaluation, imaging data were not available for standardized remeasurements in most cases. Cases underwent targeted sequencing of genes associated with HCM, as per local practice at the time of analysis. Rare variants detected through sequencing in each of the contributing cohorts of this study were assessed centrally for pathogenicity according to the American College of Medical Genetics and Genomics and the Association for Molecular Pathology (ACMG/AMP) guidelines[25], using an adapted version of the CardioClassifier resource[26] (details provided in the Supplementary Note, and classification results in Supplementary Table 2).

GWAS analysis design. Quality control (QC) and case–control association analysis were performed in three strata (Netherlands, NL; Royal Brompton and Harefield Hospitals, RBH; and Canada, CAN) followed by meta-analysis. See Supplementary Note for details regarding each stratum, including enrolling centers, DNA genotyping, QC and imputation.

Association analysis. The association of alternate allele dosage with HCM was performed for each of the three strata using a frequentist test in an additive model implemented in SNPTEST (v.2.5.2 for the CAN and NL strata, v.2.5.4 for the RBH stratum), correcting for the first three genotypic principal components. The results of the three strata were then combined using an IVW fixed-effect meta-analysis, performing meta-analysis heterogeneity analysis, implemented in METAL[27] (version released on 25 March 2011). SNPs that were missing in any of the three strata, as well as those with a heterogeneity test $P < 0.05$, were excluded. The stringent exclusion *P*-value threshold for meta-analysis heterogeneity test was necessary to exclude most common SNPs that tag one of the population-specific founder HCM-causing pathogenic variants (for example, NM_000256.3 (*MYBPC3*): c.2373dup (p.Trp792fs) in the Dutch population; NM_000364.4 (*TNNT2*): c.881 G>A (p.Trp294Ter) in French Canadians). A subgroup analysis restricted to HCM cases without founder variants in *MYBPC3* was performed. For the sake of this analysis, a founder variant was defined as a rare variant classified as pathogenic or likely pathogenic that was observed at least 10 times in the case cohort combining all strata. Using this definition, HCM cases carrying the following *MYBPC3* variants (ENST00000545968) were excluded from this analysis: c.2373dupG, c.2827 C>T, c.2864_2865delCT, c.3776delA, c.481 C>T, c.551dupT, c.927-2 A>G. Variant c.551dupT is a French Canadian founder while all others are Dutch founders. The summary results of this subanalysis are shown in Supplementary Fig. 1. The results of the main HCM case–control meta-analysis are shown in Fig. 2, Table 1 and Supplementary Table 4. QQ plots of each stratum and forest plots for lead SNPs at all significant loci are shown in Supplementary Fig. 2.

Analysis of heritability attributable to common variants. We used the GREML approach of GCTA (v.1.92.4 beta)[4,28] to estimate how much of the variance in HCM susceptibility could be attributed to common genetic variants (SNP-based heritability, h^2_{SNP}). The analysis was performed by stratum (NL, RBH, CAN), followed by a fixed-effects and random effects meta-analysis using the *meta* package (v.4.9-9) in R v.3.6.0. Before heritability analyses, we performed additional stringent postimputation QC as suggested[29], using hard call genotypes (genotype probability, GP > 0.9) and excluding SNPs with missing rate >0.01, MAF < 0.05, Hardy–Weinberg test $P < 0.05$ and phenotype biased missingness $P < 0.05$, as well as samples with missing rate >0.01, and excluded regions in the genome that tag founder HCM-causing rare variants in HCM (chr11:42008264–65380094 (*MYBPC3*) in NL and CAN, and chr1: 196816127–204926893 (*TNNT2*) in CAN). We then generated a genetic relationship matrix (GRM) and excluded distantly related individuals (proportion identity by descent, IBD > 0.05). We estimated h^2_{SNP} on the liability scale assuming a prevalence of 0.2% (ref. [3]) with the first 10 genotypic principal components and sex as covariates. In addition to standard GREML, we also performed GREML-LDMS[5] with 200-kb segmentation, stratification of SNPs in four sets by LD scores of individual SNPs in R followed by GRM estimation per SNP stratum and REML analysis with multiple GRMs. To estimate the h^2_{SNP} specific to the previously published locus (near *FHOD3*), the 15 novel loci and the rest of the genome, we also performed partitioned heritability analysis using GREML, using the same QC and prevalence described for overall h^2_{SNP}. The genome was partitioned into three segments (*FHOD3* locus, 15 novel loci and rest of genome). Loci were defined based on the lead SNP ± 500 kb. Analysis was also performed by stratum, followed by an IVW meta-analysis using fixed-effects and random effects models. The results of h^2_{SNP} estimation are shown in Supplementary Table 3.

HCM GWAS replication dataset. Replication of HCM loci reaching the significance threshold was tested in an independent dataset comprising 2,694 HCM cases included from the HCMR[17] or the NIHR BRRD[18], and 47,486 controls without HCM included from the UKBB or BRRD. The detailed methodology is described in Harper et al.[16] Of the 2,780 HCM cases included in Harper et al.[16], 86 are overlapping with the present discovery dataset and have been excluded from the replication dataset. The results of this replication analysis and a fixed-effects model meta-analysis combining the discovery and replication results are shown in Supplementary Table 10.

Meta-analysis of association studies in DCM. A meta-analysis of three published case–control association studies[7–9] of DCM was performed. The included studies are described in the Supplementary Note and in Supplementary Table 5. A fixed-effects meta-analysis was performed using METAL[27] (version released on 25 March 2011). Study weighting was performed using the case sample size. The results of the DCM meta-analysis are shown in Extended Data Fig. 1 and Supplementary Table 7. QQ plots for each study and forest plots for the lead SNPs at all significant loci are shown in Supplementary Fig. 7.

GWAS of CMR-derived LV traits. *UKBB study population.* The UKBB is an open-access population cohort resource that has recruited half a million participants in its initial recruitment phase, from 2006 to 2010. At the time of analysis, robust CMR imaging data were available from 26,523 individuals in the imaging substudy. The UKBB CMR acquisition protocol has been described previously[30]. In brief, images were acquired according to a basic cardiac imaging protocol using clinical 1.5-Tesla-wide bore scanners (MAGNETOM Aera, Syngo Platform VD13A, Siemens Healthcare, Erlangen, Germany) in three separate imaging centers. Extensive clinical and questionnaire data and genotypes are available for these individuals. Clinical data were obtained at the time of the imaging visit. These included sex (31), age (21,003), weight (21,002), height (50), systolic blood pressure (SBP) (4,080), diastolic blood pressure (DBP) (4,079), self-reported noncancer illness codes (20,002) and ICD-10 codes (41,270). The mean age at the time of CMR was 63 ± 8 years (range 45–80) and 46% of participants were male. Cohort anthropometrics, demographics and comorbidities are reported in Supplementary Table 6. Exclusion criteria for the UKBB imaging substudy included childhood disease, pregnancy and contraindications to magnetic resonance imaging scanning. For the current analysis, we also excluded, by ICD-10 code and/or self-reported diagnoses, any participants with heart failure, cardiomyopathy, a previous myocardial infarction or structural heart disease. We also excluded those with uncontrolled hypertension (defined by SBP or DBP > 180 mmHg or > 110 mmHg, respectively, at time of imaging visit) or with extremes of body mass index (BMI < 16 or > 40). We restricted our analysis to individuals of European ancestry defined by genotype as described (http://www.ukbiobank.ac.uk/wp-content/uploads/2014/04/UKBiobank_genotyping_QC_documentation-web.pdf). After phenotyping, we also excluded participants with meanWT > 13 mm in any of the 16 American Heart Association (AHA) LV segments[31] and participants with outlying (>3 SD from mean) LV mass, LV volumes or LV ejection fraction. The UKBB received National Research Ethics Approval (REC reference 11/NW/0382). All participants provided informed consent (https://biobank.ctsu.ox.ac.uk/crystal/crystal/docs/Consent.pdf). The present study was conducted under terms of UKBB access approval 18545.

LV trait phenotyping. A description of CMR image analysis appears in the Supplementary Note and Supplementary Fig. 3. We included nine LV phenotypes for GWAS analyses: LVEDV, LVESV, LVEF, LVM, concentricity (LVconc = LVM/LVEDV) and meanWT, as well as global peak strain in radial ($strain^{rad}$), longitudinal ($strain^{long}$) and circumferential ($strain^{circ}$) directions. The mean and SD of all nine LV phenotypes overall and stratified by sex are shown in Supplementary Table 6. The distributions of raw measures of these nine phenotypes are shown in Supplementary Fig. 4. Despite non-normal distribution of some of the raw LV phenotypes, the residuals from our regression model including covariates (as defined below) approximated to normal distributions for all phenotypes (Supplementary Fig. 5). Therefore, the primary analysis was conducted using raw, non-normalized phenotypes.

LV trait genome-wide association analyses. A description of genotyping, imputation and QC appears in the Supplementary Note. The GWAS model included age, sex, height, weight and mean arterial pressure (MAP) as covariates. We performed a meta-analysis comprising two strata. Participants recruited and imaged in the North of England (Cheadle, Newcastle) were treated as the first stratum ($n = 15{,}215$ after exclusions) and those recruited in the South of England (Reading) comprised the second stratum ($n = 4{,}045$). For each stratum, BOLT–LMM[32] (v.2.3.2) was used to construct mixed models for association with around 9.5 million directly

genotyped and imputed SNPs. A high-quality set of directly genotyped model SNPs was selected to account for random effects in the genetic association analyses. These were selected by MAF (>0.001) and LD-pruned ($r^2 < 0.8$) to create an optimum SNP set size of around 500,000. The model was then applied to the >9.8 million imputed SNPs passing QC and filtering. IVW meta-analysis was carried out with summary statistics from both strata using METAL[27] (version released on 25 March 2011). The results of the LV traits GWAS are shown in Supplementary Table 8 and Extended Data Figs. 2–10.

GWAS statistical significance threshold. We accounted for multiple testing to define the *P*-value threshold for genome-wide statistical significance in the HCM, DCM and LV traits GWAS. As expected, LV trait pairs are phenotypically correlated (Supplementary Table 9). Supplementary Fig. 6 displays a phenotypic correlation heatmap using absolute values with dendrograms constructed using Euclidean distance and complete hierarchical clustering. Cutting the dendrogram at a height of 1.5 results in three LV phenotype clusters (Supplementary Fig. 6): (1) a contractility cluster comprising $strain^{long}$, $strain^{circ}$, $strain^{rad}$ and LVEF; (2) a LV volume cluster comprising LVEDV and LVESV; and (3) a LV hypertrophy cluster comprising LVM, meanWT and LVconc. The genome-wide significance threshold for the GWAS of LV traits, HCM and DCM was therefore set to $P < 1 \times 10^{-8}$ ($5 \times 10^{-8}/5$; accounting for three LV clusters + DCM + HCM).

Pairwise genetic correlation. We performed pairwise genetic correlation between HCM, DCM and the nine LV traits using LD score correlation (LDSC, v.1.0.1)[13,14]. For each GWAS, we first reformatted summary statistics using the 'munge_sumstats.py' command, filtering for the HapMap3 SNPs with corresponding alleles using the --merge-alleles w_hm3.snplist flag, as recommended. The HapMap3 SNPs were downloaded from https://data.broadinstitute.org/alkesgroup/LDSCORE/w_hm3.snplist.bz2. We then assessed genetic correlation for each of the 55 pairs (HCM, DCM and nine LV traits) using the ldsc.py --rg command and precomputed LD scores from the European 1000 Genomes Project dataset, which were downloaded from https://data.broadinstitute.org/alkesgroup/LDSCORE/eur_w_ld_chr.tar.bz2. We did not constrain the single-trait and cross-trait LD score regression intercepts. The results of the genetic correlation analyses are shown in Fig. 3 and Supplementary Table 9.

Multi-trait analysis of GWAS. We performed multi-trait analysis of GWAS summary statistics using MTAG (v.1.0.8)[15] to increase power for discovery of genetic loci associated with HCM, DCM and LV traits. MTAG uncovers genetic loci associated with a phenotype when the standard single-trait GWAS is underpowered. By definition, it will uncover new genetic loci whenever these are associated with the other phenotypes included. It may theoretically fail to identify phenotype-specific loci. Two MTAG analyses were performed, one only including the summary statistics of the nine LV traits (referred to as 'MTAG9'), and another one including the summary statistics of the nine LV traits, HCM and DCM (referred to as 'MTAG11'). Specifically, MTAG9 was used for additional locus discovery for the nine LV traits, and MTAG11 was used for additional locus discovery for HCM and DCM. Only SNPs included in all meta-analyses (that is HCM, DCM and LV traits) were used in MTAG. The coded/noncoded alleles were aligned for all 11 studies before MTAG, and multi-allelic SNPs were removed. All summary statistics refer to the positive strand of GRCh37 and, as such, ambiguous/palindromic SNPs (having alleles A/T or C/G) were not excluded. Regression coefficients (beta) and their standard errors were used for MTAG9, and *Z*-scores were used for MTAG11 (since regression coefficients and standard errors were not directly available in all included DCM studies). The results of the multi-trait analyses are shown as panels **b** in Fig. 2 and Extended Data Figs. 1–10, as well as Supplementary Tables 4, 7 and 8.

Two-sample MR. We assessed whether increased contractility is causally linked to increased HCM risk using two-sample MR using LV contractility parameters as exposure variables and HCM as an outcome. Two-sample MR was performed using the *TwoSampleMR* (MRbase) package[33] (v.0.4.25) in R v.3.6.0. Four exposure variables corresponding to measures of LV contractility were used separately: LVEF as a volumetric marker of contractility, and global strain (circumferential ($strain^{circ}$), radial ($strain^{rad}$) and longitudinal ($strain^{long}$)) as contractility markers based on myocardial tissue deformation. We used two approaches for instrument SNP selection: (1) $P < 5 \times 10^{-8}$ in the single LV trait analysis and (2) $P < 5 \times 10^{-8}$ in the MTAG9 analysis (that is, excluding HCM and DCM). Only independent SNPs (using $r^2 < 0.01$ in the European 1000 Genomes population) were included. The outcome summary statistics were those of the single-trait HCM case–control meta-analysis. Insertions/deletions and palindromic SNPs with intermediate allele frequencies (MAF > 0.42) were excluded, and other SNPs in the same locus were included only if reaching the *P*-value threshold for instrument SNP selection. The SNPs included in MR analyses and their effects in the exposure and outcome studies are shown in Supplementary Table 11. IVW was used as a primary analysis. We used three additional methods as sensitivity analyses: weighted median[34], weighted mode[35] and robust adjusted profile score (RAPS)[36]. RAPS was used with the default parameters (over.dispersion = TRUE and loss.function = 'tukey'). MR–Egger[37] was not used given the limited number of SNP instruments. Cochran's *Q* statistics were calculated to investigate heterogeneity between SNP causal effects using IVW. Evidence of directional pleiotropy was also assessed using the MR–Egger intercept. Mean *F*-statistics were calculated to assess the strength of the genetic instruments used. Leave-one-out analysis was also performed to ensure the SNP causal effects are not driven by a particular SNP. We also performed a secondary analysis using the generalized summary-data-based Mendelian randomization (GSMR) implemented in GCTA (v.1.92.4 beta)[38]. LD estimation was performed using the European samples from the 1000 Genomes Project reference dataset. As for the analysis using TwoSampleMR, instrument SNPs were selected using two approaches (see (1) and (2) above). The default parameters were used, with the following exceptions: the r^2 clumping threshold was changed to 0.01 and the minimum number of SNPs required was changed to 5. Removal of pleiotropic SNPs was performed as suggested using the GSMR-implemented HEIDI outlier algorithm with default parameters[38]. The results of the MR are shown in Supplementary Table 12, with effect plots and leave-one-out analyses shown in Supplementary Figs. 8 and 9, respectively.

Genome-wide visualization and annotation. Summary statistics for all single-trait and multi-trait analyses were uploaded to FUMA (Functional Mapping and Annotation of GWAS, v.1.3.5)[39] for visualization and genome-wide analyses. Manhattan and QQ plots were constructed. Gene-set and tissue expression analyses were performed using MAGMA[19] v.1.07, as implemented in FUMA. We used Gene Ontology (GO) gene sets from the Molecular Signatures Database (MSigDB, v.6.2)[40] for the gene-set analysis and the Genotype-Tissue Expression project (GTEx[41] v.8) for the tissue specificity analysis. The results of MAGMA analyses using the HCM and DCM MTAG summary statistics are shown in Supplementary Tables 13 and 14 (gene-set analyses) and Supplementary Fig. 10 (tissue specificity analyses).

Locus annotation. All loci associated with HCM, DCM and LV traits in the single-trait or multi-trait analyses were annotated using lookup for: (1) proxy coding variants (Supplementary Table 15), (2) cis-eQTL (Supplementary Table 16), (3) cis-sQTL (Supplementary Table 17) and (4) contact with gene promoters using Hi-C (Supplementary Table 18). We also assessed whether GWAS loci colocalize with genes associated with Mendelian cardiomyopathy and performed cross-traits lookups for all HCM, DCM and LV traits loci (Fig. 4 and Supplementary Tables 4, 7 and 8). See Supplementary Note for methodological details.

Association of PRS_{HCM} with phenotypic manifestation in sarcomeric variant carriers. We sought to assess whether a common variant PRS derived from the HCM case–control GWAS (PRS_{HCM}) accounts for phenotypic variability and severity in pathogenic or likely pathogenic variant carriers.

Study population. In this analysis, we included probands and family members that carry pathogenic or likely pathogenic variants associated with HCM from the Erasmus Medical Center (EMC). All variants were centrally curated as described in the Supplementary Note, and only participants that carry (likely) pathogenic variants were included (see list in Supplementary Table 2). Homozygous carriers and those carrying multiple pathogenic or likely pathogenic variants were excluded. Clinical data including maxLVWT on cardiac imaging and time of clinical events were retrieved from an ongoing registry[42,43], including all patients with HCM and their relatives at the EMC. Missing data were collected from chart review. The baseline characteristics of the study population are shown in Supplementary Table 20.

Derivation of PRS_{HCM}. The PRS_{HCM} was derived from an independent GWAS, excluding HCM cases with (likely) pathogenic variants from EMC. This was done to ensure that the PRS is derived from an independent cohort. Specifically, a Dutch HCM case–control GWAS was repeated after excluding 161 cases from EMC cases that carry (likely) pathogenic variants, followed by a meta-analysis combined with the RBH HCM GWAS and the CAN HCM GWAS, followed by MTAG11 as described above. Lead SNPs reaching the genome-wide significance threshold ($P < 5 \times 10^{-8}$) were included in the PRS_{HCM}. Those SNPs included in the PRS_{HCM} and their corresponding weights are shown in Supplementary Table 19.

Calculation of PRS_{HCM}. All EMC samples that carry pathogenic or likely pathogenic HCM variants underwent array genotyping on the Illumina GSA. QC was performed as described in the Supplementary Note for the Dutch HCM GWAS, except for IBD analysis, where only duplicate (or twin) samples were excluded. No sample was excluded for relatedness, which was accounted for using a GRM as described in the statistical analyses paragraph below. Imputation and postimputation QC were performed also as described for the GWAS in the Supplementary Note. PRS_{HCM} was calculated by summing the products of each lead risk allele dosage by the corresponding regression coefficient in the derivation study (Supplementary Table 19) using Plink 2.0, followed by scaling to a mean of 0 and SD of 1.

Study endpoints. Two primary endpoints were predefined. The first primary endpoint was maxLVWT at last available transthoracic echocardiogram (TTE) or

CMR. MaxLVWT is routinely assessed in clinical practice as a measure of HCM severity and for risk stratification of life-threatening ventricular arrhythmias[3]. For participants who had cardiac transplantation and/or septal reduction therapy to relieve LV obstruction, the last available CMR or TTE before cardiac transplantation and/or septal reduction therapy was used. Considering the higher accuracy of CMR to assess wall thickness in all LV segments, maxLVWT from CMR was used whenever available unless TTE was performed more than 5 years after last CMR. To account for body size, a determinant of wall thickness in the general population[44] and in HCM[45], maxLVWT was indexed to BSA calculated using the DuBois formula ($0.007184 \times \text{height (cm)}^{0.725} \times \text{weight (kg)}^{0.425}$). The second primary endpoint was time to first adverse clinical event (a composite of invasive septal reduction therapy, cardiac transplantation, sustained ventricular arrhythmia, sudden cardiac death, appropriate defibrillator therapy or atrial fibrillation/flutter). The components of this composite endpoint were also assessed as secondary endpoints. As a sensitivity analysis, we also performed an analysis for the primary outcomes restricted to nonprobands.

Statistical analyses. A GRM was estimated using GCTA (v.1.92.4 beta) and used to account for between-sample relatedness. The association of PRS_{HCM} with maxLVWT indexed to BSA (in $mm\,m^{-2}$) was performed using a mixed linear model integrating the GRM as a random effect. Neither sex nor rare variant type (*MYBPC3* truncation versus others) were associated with maxLVWT and were therefore not included as covariates. The association of PRS_{HCM} with the primary composite clinical events endpoint and secondary endpoints were assessed using a Cox proportional hazards mixed effects model integrating the GRM as a random effect. Since biological male sex was significantly associated with increased risk for clinical events, it was added as a fixed-effect covariate. Time 0 was set to birth in the Cox model to maximize statistical power by including events that occurred at the time of first medical encounter. Given the genetic nature of our exposure factor, all study participants are exposed since birth. Nevertheless, there is a possibility of selection bias in our cohort, since study participants have to reach the age of inclusion. Study participants were censored at the time of last clinical follow up. For analyses of secondary endpoints that do not include cardiac transplantation, study participants were also censored at the time of cardiac transplantation. In addition to PRS_{HCM}, we also assessed the association of a genome-wide score (PRS_{AF}) derived from a large atrial fibrillation meta-analysis and validated by Khera et al.[46] with atrial fibrillation within the study population. Mixed effects analyses of PRS_{HCM} with maxLVWT was performed using the *lmekin* and mixed effects analyses of PRS_{HCM} and PRS_{AF} with clinical events was performed using the *coxme* function, both from the *coxme* package v.2.2-14 in R v.3.6.0. The statistical significance threshold was set to $P < 0.025$ for the primary endpoints (0.05/2 primary endpoints) and $P < 0.05$ for hypothesis-generating secondary endpoints. The results of the primary, secondary and sensitivity analyses are shown in Supplementary Table 21. Kaplan–Meier curves stratified by PRS_{HCM} above or below the median are shown in Fig. 5.

Reporting Summary. Further information on research design is available in the Nature Research Reporting Summary linked to this article.

Data availability

Data from the Genome Aggregation Database (gnomAD, v.2.1) are available at https://gnomad.broadinstitute.org. Data from the UKBB participants can be requested from the UKBB Access Management System (https://bbams.ndph.ox.ac.uk). Data from the GTEx consortium are available at the GTEx portal (https://gtexportal.org). Other datasets generated during and/or analyzed during the current study can be made available upon reasonable request to the corresponding authors. Individual level data sharing is subject to restrictions imposed by patient consent and local ethics review boards. Results from meta-analyses of GWAS reported in this article are available at https://www.heart-institute.nl/gwas and https://data.hpc.imperial.ac.uk (https://doi.org/10.14469/hpc/7468).

References

25. Richards, S. et al. Standards and guidelines for the interpretation of sequence variants: a joint consensus recommendation of the American College of Medical Genetics and Genomics and the Association for Molecular Pathology. *Genet. Med.* **17**, 405–424 (2015).
26. Whiffin, N. et al. CardioClassifier: disease- and gene-specific computational decision support for clinical genome interpretation. *Genet. Med.* **20**, 1246–1254 (2018).
27. Willer, C. J., Li, Y. & Abecasis, G. R. METAL: fast and efficient meta-analysis of genomewide association scans. *Bioinformatics* **26**, 2190–2191 (2010).
28. Yang, J., Lee, S. H., Goddard, M. E. & Visscher, P. M. GCTA: a tool for genome-wide complex trait analysis. *Am. J. Hum. Genet.* **88**, 76–82 (2011).
29. Lee, S. H., Wray, N. R., Goddard, M. E. & Visscher, P. M. Estimating missing heritability for disease from genome-wide association studies. *Am. J. Hum. Genet.* **88**, 294–305 (2011).
30. Petersen, S. E. et al. UK Biobank's cardiovascular magnetic resonance protocol. *J. Cardiovasc. Magn. Reson.* **18**, 8 (2016).
31. Cerqueira, M. D. et al. Standardized myocardial segmentation and nomenclature for tomographic imaging of the heart. A statement for healthcare professionals from the Cardiac Imaging Committee of the Council on Clinical Cardiology of the American Heart Association. *Circulation* **105**, 539–542 (2002).
32. Loh, P. R. et al. Efficient Bayesian mixed-model analysis increases association power in large cohorts. *Nat. Genet.* **47**, 284–290 (2015).
33. Hemani, G. et al. The MR-Base platform supports systematic causal inference across the human phenome. *eLife* **7**, e34408 (2018).
34. Bowden, J., Davey Smith, G., Haycock, P. C. & Burgess, S. Consistent estimation in Mendelian randomization with some invalid instruments using a weighted median estimator. *Genet. Epidemiol.* **40**, 304–314 (2016).
35. Hartwig, F. P., Davey Smith, G. & Bowden, J. Robust inference in summary data Mendelian randomization via the zero modal pleiotropy assumption. *Int. J. Epidemiol.* **46**, 1985–1998 (2017).
36. Zhao, Q., Wang, J., Hemani, G., Bowden, J. & Small, D. S. Statistical inference in two-sample summary-data Mendelian randomization using robust adjusted profile score. *Ann. Statist.* **48**, 1742–1769 (2020).
37. Bowden, J., Davey Smith, G. & Burgess, S. Mendelian randomization with invalid instruments: effect estimation and bias detection through Egger regression. *Int. J. Epidemiol.* **44**, 512–525 (2015).
38. Zhu, Z. et al. Causal associations between risk factors and common diseases inferred from GWAS summary data. *Nat. Commun.* **9**, 224 (2018).
39. Watanabe, K., Taskesen, E., van Bochoven, A. & Posthuma, D. Functional mapping and annotation of genetic associations with FUMA. *Nat. Commun.* **8**, 1826 (2017).
40. Subramanian, A. et al. Gene set enrichment analysis: a knowledge-based approach for interpreting genome-wide expression profiles. *Proc. Natl Acad. Sci. USA* **102**, 15545–15550 (2005).
41. GTEx Consortium. Genetic effects on gene expression across human tissues. *Nature* **550**, 204–213 (2017).
42. van Velzen, H. G. et al. Effect of gender and genetic mutations on outcomes in patients with hypertrophic cardiomyopathy. *Am. J. Cardiol.* **122**, 1947–1954 (2018).
43. Vriesendorp, P. A. et al. Long-term outcomes after medical and invasive treatment in patients with hypertrophic cardiomyopathy. *JACC Heart Fail.* **2**, 630–636 (2014).
44. LaBounty, T. M., Bach, D. S., Bossone, E. & Kolias, T. J. Indexing left ventricular wall thickness to body surface area improves prognostic value. *Echocardiography* **36**, 824–830 (2019).
45. Huurman, R. et al. Effect of body surface area and gender on wall thickness thresholds in hypertrophic cardiomyopathy. *Neth. Heart J.* **28**, 37–43 (2020).
46. Khera, A. V. et al. Genome-wide polygenic scores for common diseases identify individuals with risk equivalent to monogenic mutations. *Nat. Genet.* **50**, 1219–1224 (2018).

Acknowledgements

R.T. received funding from the Canadian Heart Rhythm Society (George Mines Award), the European Society of Cardiology (Research fellowship grant), the Canadian Institutes of Health Research (funding reference number 169063) and the Fonds de Recherche du Québec—Santé (reference number 135055). R.T. and J.C.-T. received support from the Philippa and Marvin Carsley Cardiology Chair. C.F. received funding from a British Heart Foundation Clinical Research Training Fellowship FS/15/81/31817. X.X. is currently a postdoctoral scientist funded by the Medical Research Council London Institute of Medical Sciences. A.R.H. received support from the Medical Research Council Doctoral Training Partnership. R.W. received support from an Amsterdam Cardiovascular Sciences fellowship. E.T.H. and W.P.t.R. received support from the Young Talent Program of the Dutch Heart Foundation (CVON PREDICT 2012-10). W.P.t.R. is supported by a postdoctoral fellowship CURE-PLaN (Netherlands Heart Institute) from the Leducq Foundation. J.A.O. received support from the Amsterdam UMC's PhD scholarship. A.d.M. received support from the National Institute for Health Research (NIHR) Biomedical Research Centre based at Imperial College Healthcare NHS Trust and Imperial College London; the Medical Research Council, UK; the Academy of Medical Sciences (SGL015/1006) and a Mason Medical Research Trust grant. J.H.V. received funding from the European Research Council (ERC) under the European Union's Horizon 2020 research and innovation programme (grant no 772376 - EScORIAL). E.K. received support from the German Center for Cardiovascular Research (DZHK) Rotation Grant. F.M. is supported by a postdoctoral research fellowship from the University of Florence and by the European Union Horizon 2020 framework programme (SILICOFCM, GA 777204). H.S. received support from grants from the Japan Society for the Promotion of Science (18K15410). D.S.-L. received support from UK Med-Bio. P.R. received support from the *Fédération Française de Cardiologie*. P.R. and F.A. were supported by *Ligue contre la cardiomyopathie*. E.V. and P.C. received support from the CONNY-MAEVA charitable foundation and GenMed LABEX. The study was supported by the Dutch Heart Foundation Netherlands Cardiovascular Research Initiative (CVON; PREDICT2 2018-30 to J.P.v.T., A.A.M.W. and C.R.B.; eDETECT 2015-12 to J.P.v.T. and I.C.; DOSIS 2014-40 to J.P.v.T., F.W.A., J.v.d.V., R.A.d.B. and M.M.; PRIME to Y.M.P.; and DOLPHIN-GENESIS 2017-10 to I.C.). R.A.H. is supported by the Jacob J. Wolfe Distinguished Medical Research Chair, the Edith Schulich Vinet Research Chair in Human Genetics and the Martha G.

Blackburn Chair in Cardiovascular Research, and has received operating grants from the Canadian Institutes of Health Research (Foundation award) and the Heart and Stroke Foundation of Canada (G-18-0022147). M.-P.D. holds a Canada Research Chair in Precision Medicine Data Analysis. J.-C.T. holds the Canada Research Chair in personalized medicine and the University of Montreal endowed research chair in atherosclerosis and is the principal investigator of the Montreal Heart Institute André and France Desmarais hospital cohort funded by the Montreal Heart Institute Foundation. R.T.L. is supported by a UK Research and Innovation Rutherford Fellowship. F.W.A. is supported by the UCL Hospitals NIHR Biomedical Research Centre. F.W.A. and P.C. received support from European Union's Horizon 2020 research and innovation program under the ERA-NET Co-fund action no. 680969 (ERA-CVD DETECTIN-HF), jointly funded by the Dutch Heart Foundation (2016T096) and Netherlands Organization for Health Research and Development (ZonMw). P.J.R.B. and J.S.W. are supported by a Health Innovation Challenge Fund award from the Wellcome Trust and Department of Health, UK (HICF-R6–373). D.P.O'R. is funded by the Medical Research Council, NIHR Biomedical Research Centre based at Imperial College Healthcare NHS Trust and Imperial College London, and a British Heart Foundation Program Grant (RG/19/6/34387). K.J.H.V. receives support from the Foundation Volksbond Rotterdam. M.T. receives support from the Monat foundation. G.L. is funded by the Montreal Heart Institute Foundation, the J. C. Edwards Foundation and the Canada Research Chair Program. B.M. received support from DZHK, the German Ministry of Education and Research (CaRNAtion), Informatics for Life (Klaus Tschira Foundation) and the European Union (FP7 BestAgeing), and was supported by an excellence fellowship of the Else Kröner Fresenius Foundation. P.C. received funding from PROMEX charitable foundation. H.W. has received support from the Wellcome Trust core award (090532/Z/09/Z), the BHF Centre of Research Excellence, Oxford (RE/13/1/30181), the NIHR Oxford Biomedical Research Centre and a National Heart, Lung and Blood Institute grant (U01HL117006-01A1). P.M.M. acknowledges generous personal and research support from the Edmond J. Safra Foundation and Lily Safra, an NIHR Senior Investigator Award and the UK Dementia Research Institute. J.S.W. was supported by Wellcome Trust (107469/Z/15/Z); British Heart Foundation (SP/17/11/32885; RE/18/4/34215); Medical Research Council (UK); NIHR Royal Brompton Cardiovascular Biomedical Research Unit; NIHR Imperial College Biomedical Research Centre. C.R.B. acknowledges support from the Netherlands Organization for Scientific Research (VICI fellowship, 016.150.610) and the Leducq Foundation (project 17CVD02). This research has been conducted in part using the UK Biobank Resource under Application Number 18454, and the Genotype-Tissue Expression (GTEx) Project supported by the Common Fund of the Office of the Director of the National Institutes of Health, and by National Cancer Institute (NCI), National Human Genome Research Institute (NHGRI), National Heart, Lung and Blood Institute (NHLBI), National Institute on Drug Abuse (NIDA), National Institute of Mental Health (NIMH), and National Institute of Neorological Disorders and Stroke (NINDS). This study was supported by a kind donation from family and friends of Jean-Paul Balkestein who died at 32 years of age from hypertrophic cardiomyopathy.

Author contributions

R.T., C.F., A.M.C.V., J.M.V., W.B., N.L., P.E., E.V., M.W.T.T., J.P.v.T., P.J.R.B., S.A.C., S.K.P., J.v.d.V., K.J.H.V., G.L., B.M., P.C., I.C., M.M., A.A.M.W., H.W., P.M.M., J.S.W. and C.R.B. conceived or designed elements of the study. R.T., C.F., X.X., A.M.C.V., A.R.H., R.H., K.K.B., R.W., E.T.H., W.P.t.R., R.J.B., H.G.v.V., M.A.v.S., J.M.V., J.A.O., W.B., A.d.M., L.B., J.C.K., J.H.V., E.K., A.P., A.J.B., N.W., F.M., G.S., H.S., D.S.-L., P.R., F.A., E.V., P.L., T.M., A.T., D.M., R.A.H., J.D.R., J.A., M.-P.D., J.C.-T., G.G., P.L.L'A., P.G., J.-C.T., S.M.B., R.T.L., F.W.A., P.J.R.B., S.A.C., S.K.P., D.P.O'R., M.T., G.L., Y.M.P., B.M., P.C., R.A.d.B., M.M., A.A.M.W., H.W., J.S.W. and C.R.B. acquired, analyzed or interpreted data. R.T., C.F., X.X., R.W., J.A.O., W.B., J.S.W. and C.R.B. drafted the manuscript. All authors critically revised the manuscript for important intellectual content and approved the final version.

Competing interests

M.-P.D. is author on a patent pertaining to pharmacogenomics-guided CETP inhibition (US20170233812A1), has a minor equity interest in DalCor and has received honoraria from Dalcor and Servier and research support (access to samples and data) from AstraZeneca, Pfizer, Servier, Sanofi and GlaxoSmithKline. J.-C.T. has received research grants from Amarin, AstraZeneca, DalCor, Esperion, Ionis, Sanofi and Servier; honoraria from AstraZeneca, DalCor, HLS, Sanofi and Servier; holds minor equity interest in DalCor; and is an author of a patent on pharmacogenomics-guided CETP inhibition (US20170233812A1). B.M. has received research funding from Siemens Healtheneers, Daiichi Sankyo. The UMCG, which employs R.A.d.B., has received research grants and/or fees from AstraZeneca, Abbott, Bristol-Myers Squibb, Novartis, Novo Nordisk and Roche. R.A.d.B. received speaker fees from Abbott, AstraZeneca, Novartis and Roche. HW is a consultant for Cytokinetics. P.M.M. receives an honorarium as Chair of the UKRI Medical Research Council Neuroscience and Mental Health Board. He acknowledges consultancy fees from Adelphi Communications, MedScape, Neurodiem, Nodthera, Biogen, Celgene and Roche. He has received speakers' honoraria from Celgene, Biogen, Novartis and Roche, and has received research or educational funds from Biogen, GlaxoSmithKline and Novartis. He is paid as a member of the Scientific Advisory Board for Ipsen Pharmaceuticals. J.S.W. has received research support and consultancy fees from Myokardia, Inc.

Additional information

Extended data is available for this paper at https://doi.org/10.1038/s41588-020-00762-2.

Supplementary information is available for this paper at https://doi.org/10.1038/s41588-020-00762-2.

Correspondence and requests for materials should be addressed to R.T., J.S.W. or C.R.B.

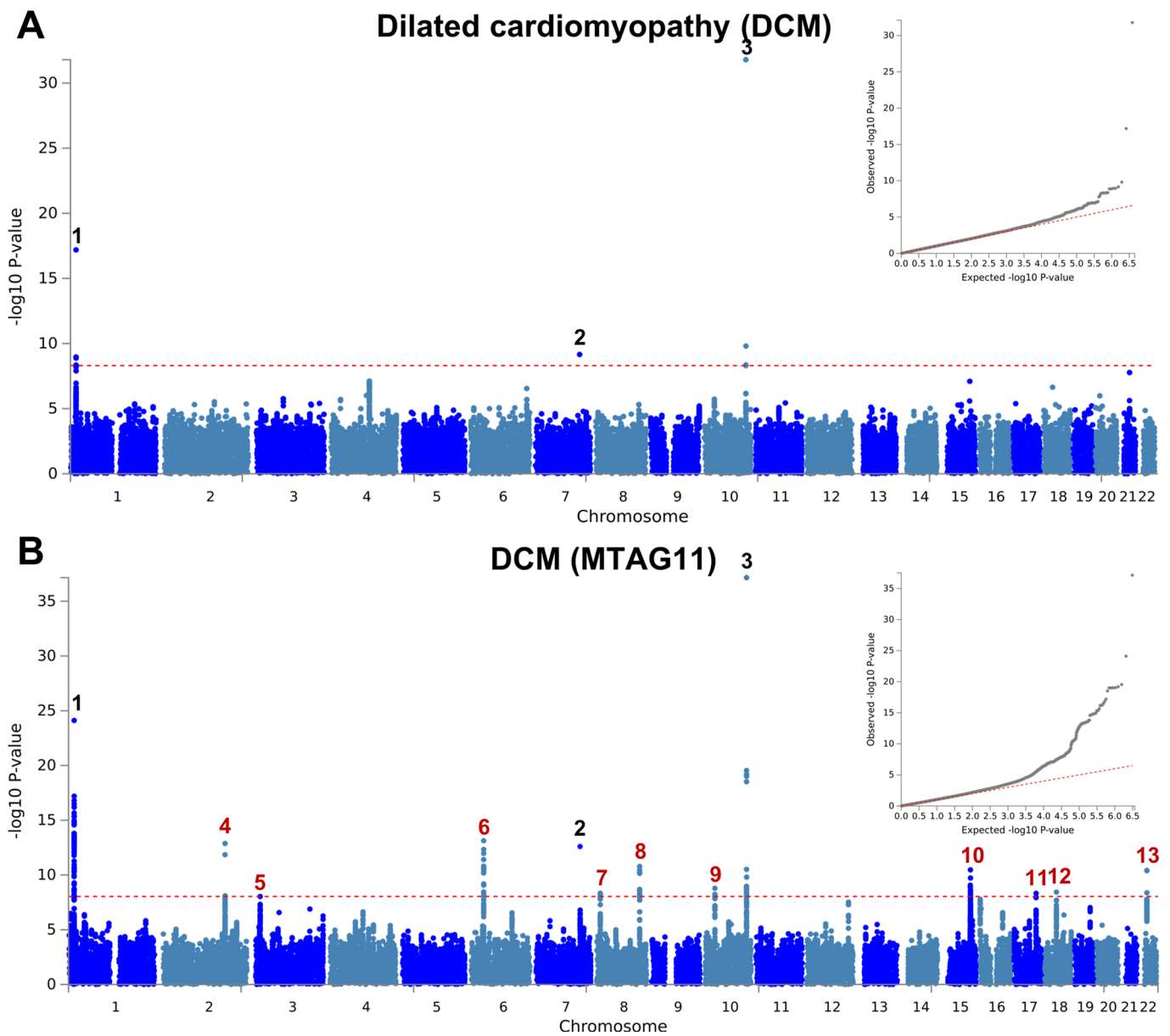

Extended Data Fig. 1 | Manhattan and QQ plots of DCM GWAS and MTAG. a,**b**, Summary results of the dilated cardiomyopathy (DCM) GWAS meta-analysis of 5,521 cases and 397,323 controls shown as Manhattan plots for the single-trait (**a**) and the multi-trait analyses (MTAG; **b**). Single-trait analysis (**a**) consisted of a fixed-effects meta-analysis of case–control GWAS using summary statistics of three previously published DCM GWAS, and multi-trait analysis results (**b**) were obtained using MTAG for DCM, including GWAS for hypertrophic cardiomyopathy (HCM) and nine left ventricular (LV) traits. Red dashed line shows the significance threshold of $P=1\times10^{-8}$. Quantile-quantile (QQ) plots shown as inserts in corresponding panels. Genomic inflation (λ) = 1.028 (single-trait) and 1.049 (MTAG). Numbering of signals as shown in Supplementary Table 7. Black numbers refer to loci reaching the statistical significance threshold in single-trait analysis, while red numbers refer to loci only reaching statistical significance in the multi-trait analysis. The low density of association signals in the single-trait analysis (**a**) is attributable to the inclusion of a large sample size study that used a low density array (Illumina Infinium HumanExome BeadChip; Supplementary Table 5).

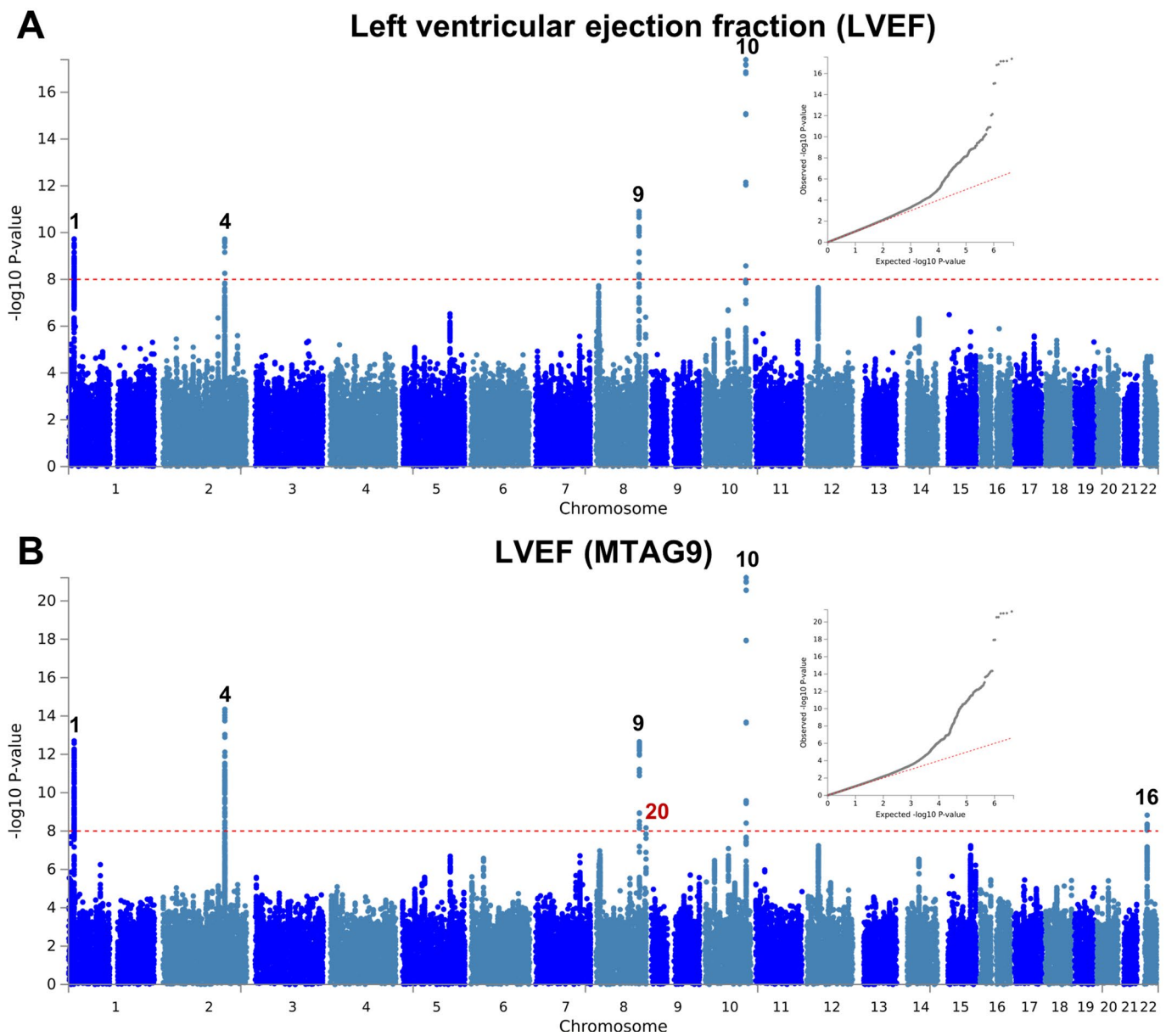

Extended Data Fig. 2 | Manhattan and QQ plots of LV ejection fraction GWAS and MTAG. a,**b**, Summary results of the left ventricular ejection fraction (LVEF) GWAS in the UK Biobank ($n = 19{,}260$) shown as Manhattan plots for the single-trait (**a**) and the multi-trait analyses (MTAG; **b**). Single-trait analysis (**a**) consisted of a fixed-effects meta-analysis of case–control GWAS using a linear mixed model (BOLT-LMM), and multi-trait analysis results (**b**) were obtained using MTAG including summary statistics for all nine left ventricular (LV) traits. Red dashed line shows the significance threshold of $P = 1 \times 10^{-8}$. Quantile-quantile (QQ) plots shown as inserts in corresponding panels. Genomic inflation (λ) = 1.041 (single-trait) and 1.049 (MTAG). Numbering of loci as shown in Supplementary Table 8. Black numbers refer to loci reaching the statistical significance threshold in any single-trait analysis, while red numbers refer to loci only reaching statistical significance in the multi-trait analysis.

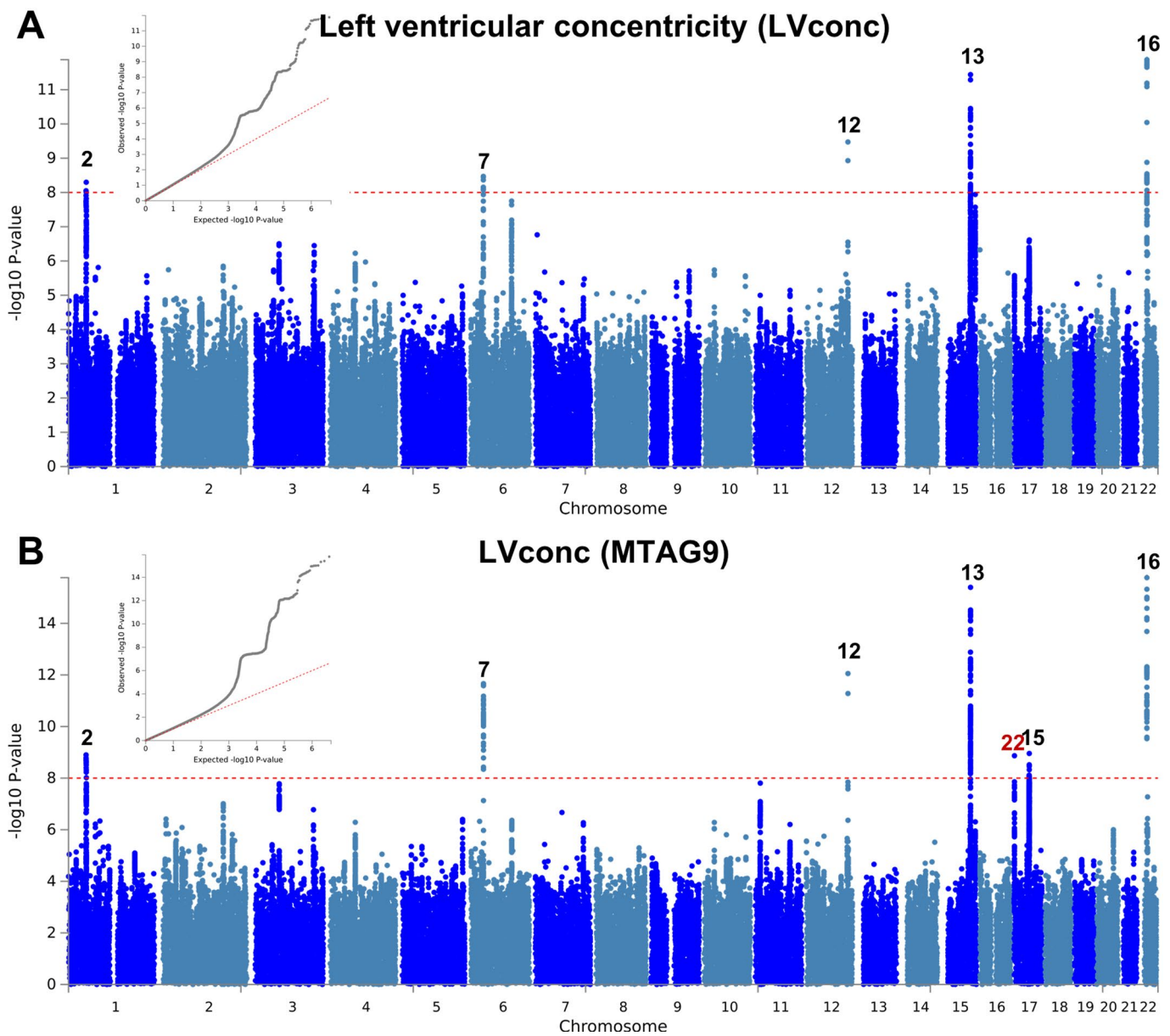

Extended Data Fig. 3 | Manhattan and QQ plots of LV concentricity GWAS and MTAG. a,**b**, Summary results of the left ventricular concentricity index (LVconc) GWAS in the UK Biobank (n=19,260) shown as Manhattan plots for the single-trait (**a**) and the multi-trait analyses (MTAG; **b**). LVconc is defined as the ratio of left ventricular mass to the left ventricular end-diastolic volume. Single-trait analysis (**a**) consisted of a fixed-effects meta-analysis of case–control GWAS using a linear mixed model (BOLT-LMM), and multi-trait analysis results (**b**) were obtained using MTAG including summary statistics for all nine left ventricular (LV) traits. Red dashed line shows the significance threshold of $P=1\times10^{-8}$. Quantile-quantile (QQ) plots shown as inserts in corresponding panels. Genomic inflation (λ)=1.06 (single-trait) and 1.084 (MTAG). Numbering of signals as shown in Supplementary Table 8. Black numbers refer to loci reaching the statistical significance threshold in any single-trait analysis, while red numbers refer to loci only reaching statistical significance in the multi-trait analysis.

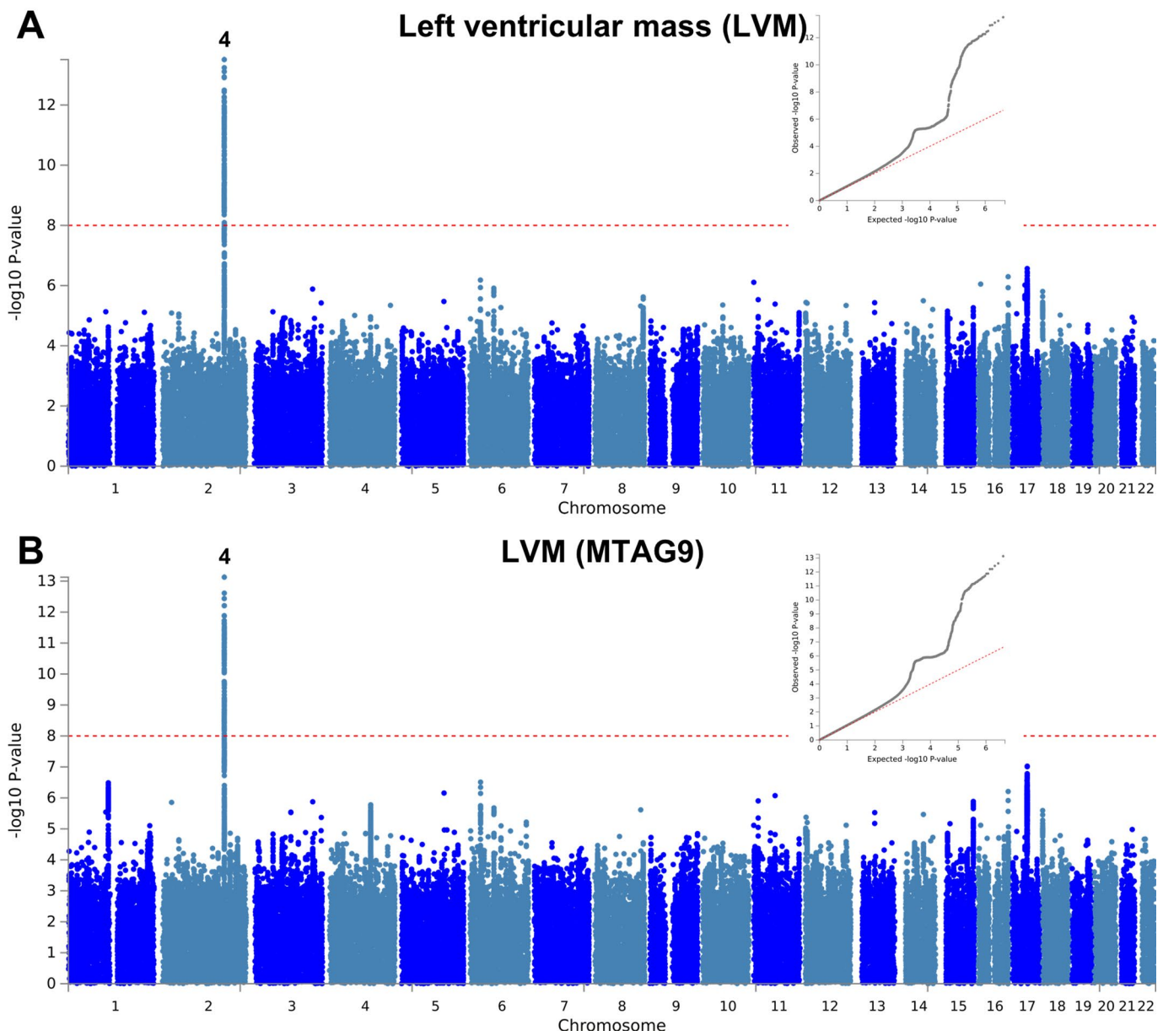

Extended Data Fig. 4 | Manhattan and QQ plots of LV mass GWAS and MTAG. a,**b**, Summary results of the left ventricular mass (LVM) GWAS in the UK Biobank ($n = 19{,}260$) shown as Manhattan plots for the single-trait (**a**) and the multi-trait analyses (MTAG; **b**). Single-trait analysis (**a**) consisted of a fixed-effects meta-analysis of case–control GWAS using a linear mixed model (BOLT-LMM), and multi-trait analysis results (**b**) were obtained using MTAG including summary statistics for all nine left ventricular (LV) traits. Red dashed line shows the significance threshold of $P = 1 \times 10^{-8}$. Quantile-quantile (QQ) plots shown as inserts in corresponding panels. Genomic inflation (λ) = 1.081 (single-trait) and 1.071 (MTAG). Numbering of signals as shown in Supplementary Table 8.

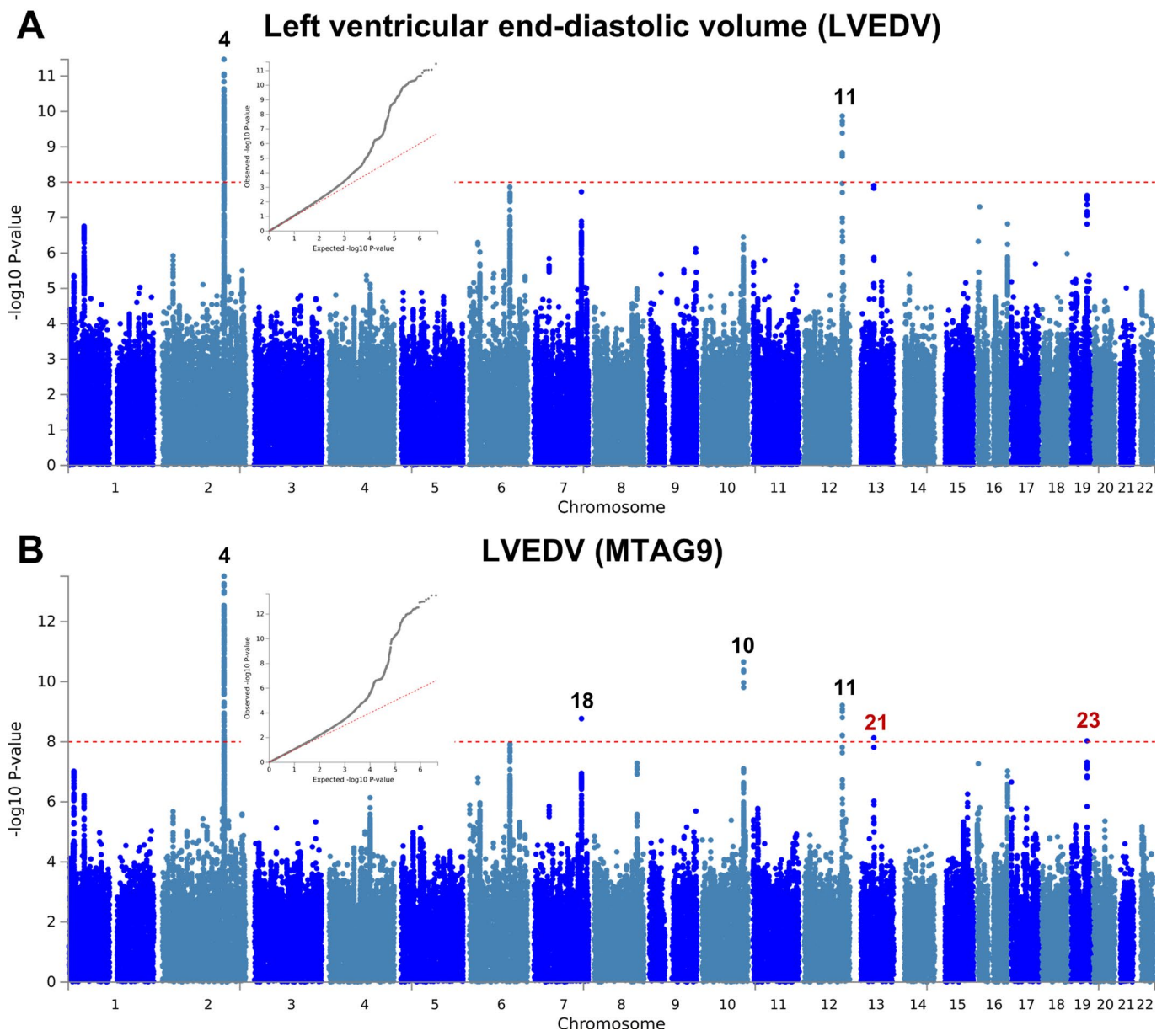

Extended Data Fig. 5 | Manhattan and QQ plots of LV end-diastolic volume GWAS and MTAG. a,**b**, Summary results of the left ventricular end-diastolic volume (LVEDV) GWAS in the UK Biobank (N=19,260) shown as Manhattan plots for the single-trait (**a**) and the multi-trait analyses (MTAG; **b**). Single-trait analysis (**a**) consisted of a fixed-effects meta-analysis of case–control GWAS using a linear mixed model (BOLT-LMM), and multi-trait analysis results (**b**) were obtained using MTAG including summary statistics for all nine left ventricular (LV) traits. Red dashed line shows the significance threshold of $P=1\times10^{-8}$. Quantile-quantile (QQ) plots shown as inserts in corresponding panels. Genomic inflation (λ) = 1.076 (single-trait) and 1.078 (MTAG). Numbering of signals as shown in Supplementary Table 8. Black numbers refer to loci reaching the statistical significance threshold in any single-trait analysis, while red numbers refer to loci only reaching statistical significance in the multi-trait analysis.

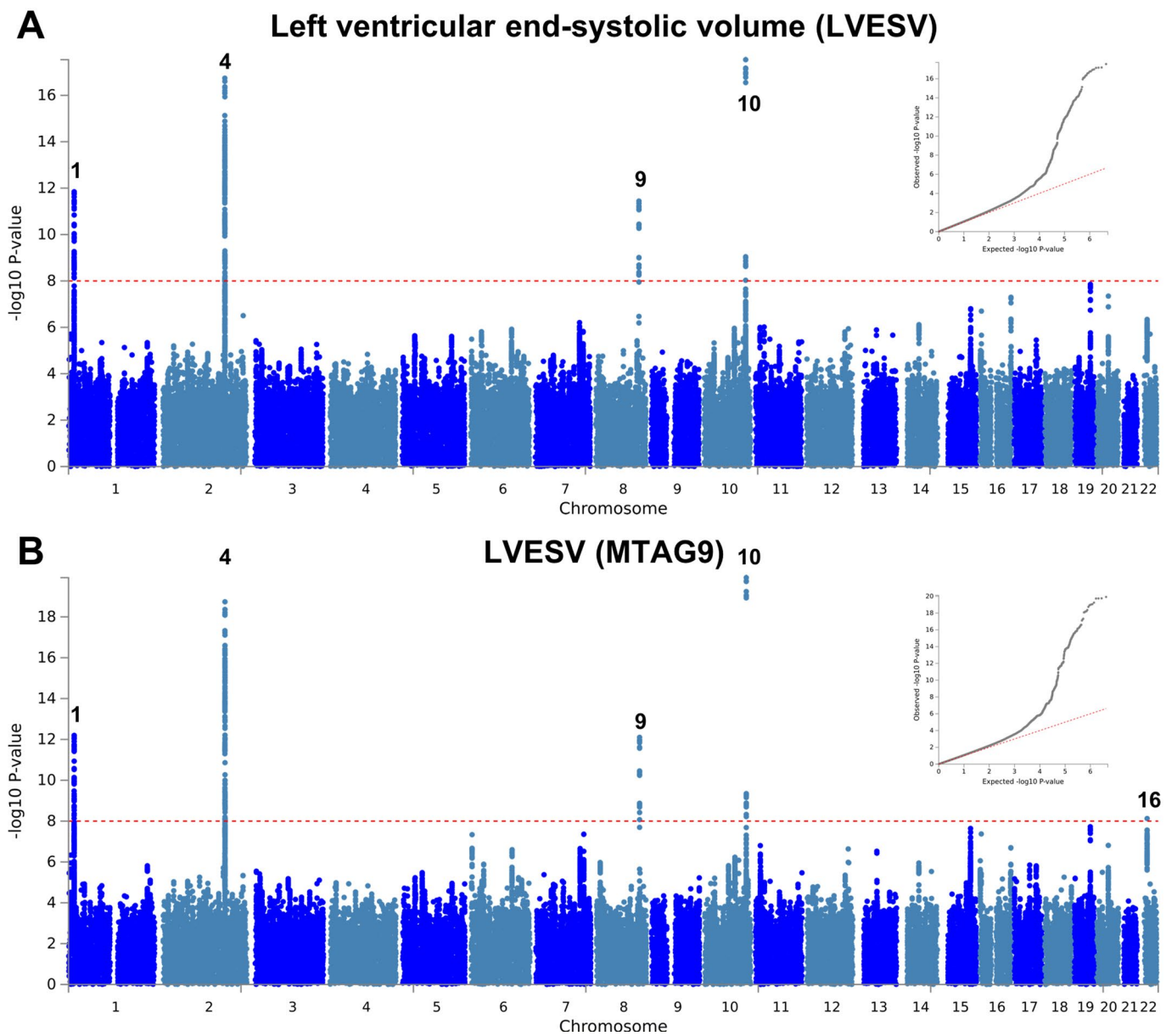

Extended Data Fig. 6 | Manhattan and QQ plots of LV end-systolic volume GWAS and MTAG. Summary results of the left ventricular end-systolic volume (LVESV) GWAS in the UK Biobank (n= 19,260) shown as Manhattan plots for the single-trait (**a**) and the multi-trait analyses (MTAG; **b**). Single-trait analysis (**a**) consisted of a fixed-effects meta-analysis of case–control GWAS using a linear mixed model (BOLT-LMM), and multi-trait analysis results (**b**) were obtained using MTAG including summary statistics for all nine left ventricular (LV) traits. Red dashed line shows the significance threshold of $P = 1 \times 10^{-8}$. Quantile-quantile (QQ) plots shown as inserts in corresponding panels. Genomic inflation (λ) = 1.069 (single-trait) and 1.081 (MTAG). Numbering of signals as shown in Supplementary Table 8.

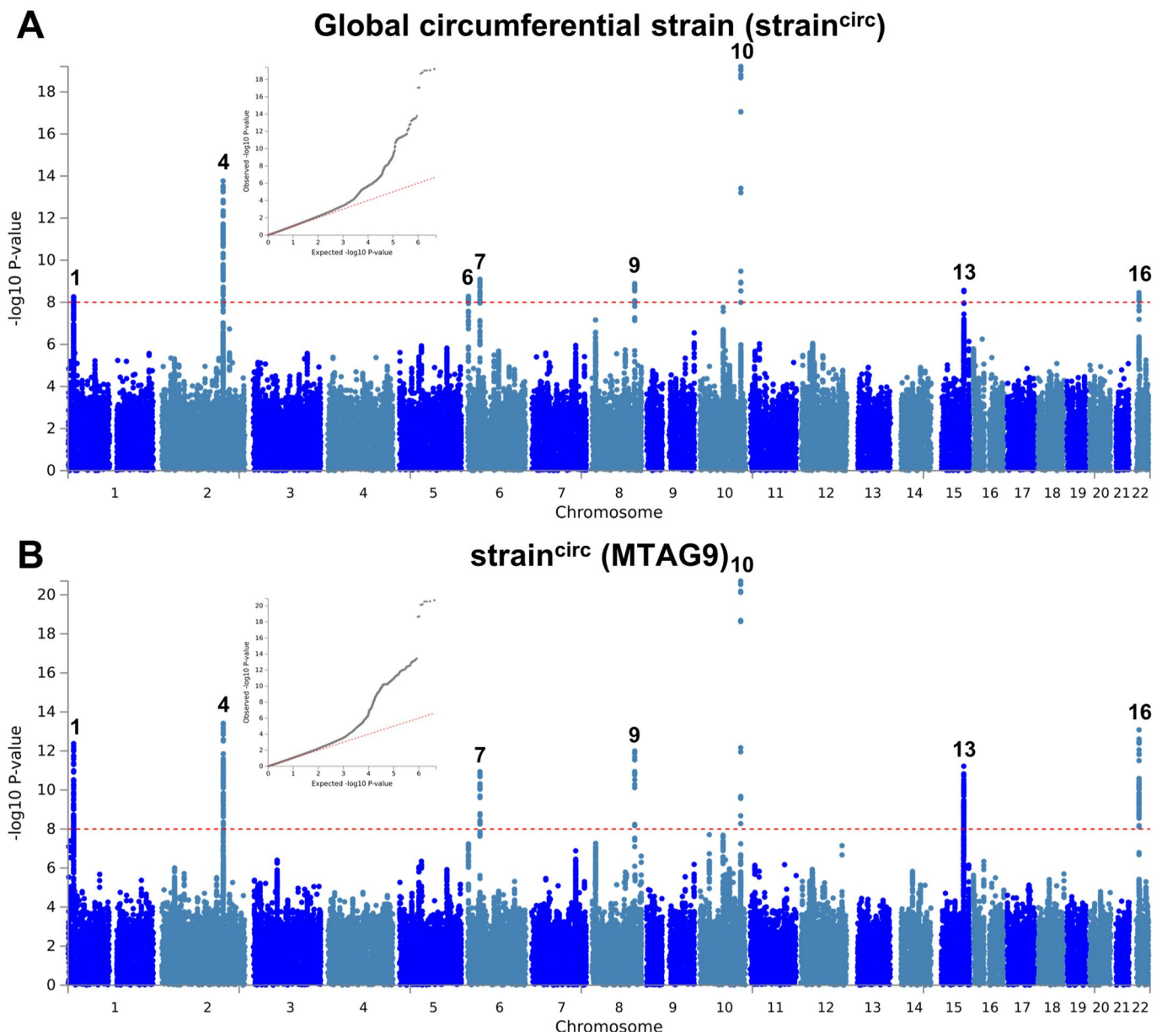

Extended Data Fig. 7 | Manhattan and QQ plots of LV global circumferential strain GWAS and MTAG. a,**b**, Summary results of the left ventricular global circumferential strain ($strain^{circ}$) GWAS in the UK Biobank (N=19,260) shown as Manhattan plots for the single-trait (**a**) and the multi-trait analyses (MTAG; **b**). Single-trait analysis (**a**) consisted of a fixed-effects meta-analysis of case–control GWAS using a linear mixed model (BOLT-LMM), and multi-trait analysis results (**b**) were obtained using MTAG including summary statistics for all nine left ventricular (LV) traits. Red dashed line shows the significance threshold of $P=1\times10^{-8}$. Quantile-quantile (QQ) plots shown as inserts in corresponding panels. Genomic inflation (λ) = 1.046 (single-trait) and 1.061 (MTAG). Numbering of signals as shown in Supplementary Table 8.

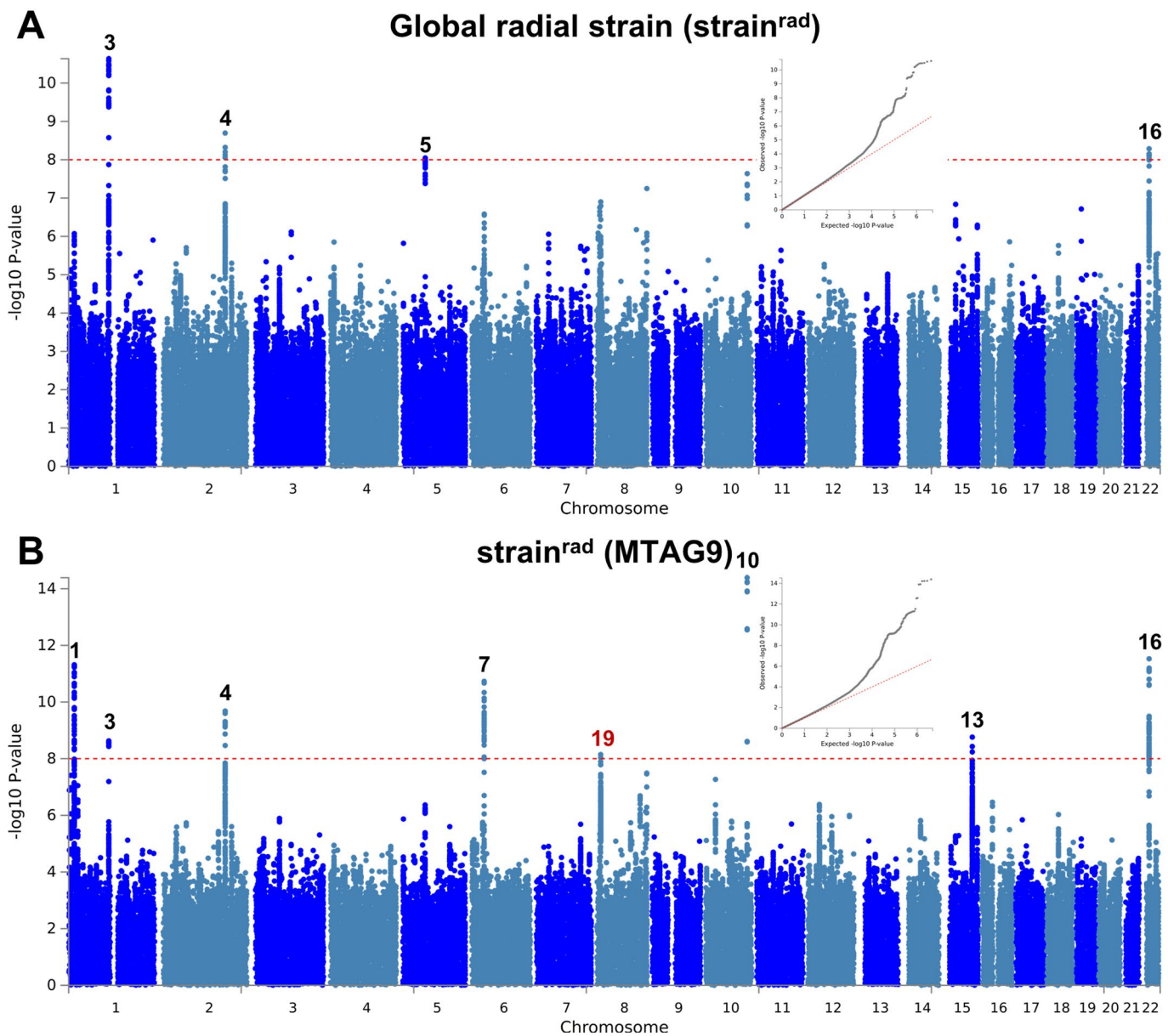

Extended Data Fig. 8 | Manhattan and QQ plots of LV global radial strain GWAS and MTAG. a,**b**, Summary results of the left ventricular global radial strain (strain^{rad}) GWAS in the UK Biobank (n=19,260) shown as Manhattan plots for the single-trait (**a**) and the multi-trait analyses (MTAG; **b**). Single-trait analysis (**a**) consisted of a fixed-effects meta-analysis of case–control GWAS using a linear mixed model (BOLT-LMM), and multi-trait analysis results (**b**) were obtained using MTAG including summary statistics for all nine left ventricular (LV) traits. Red dashed line shows the significance threshold of $P=1\times10^{-8}$. Quantile-quantile (QQ) plots shown as inserts in corresponding panels. Genomic inflation (λ)=1.049 (single-trait) and 1.057 (MTAG). Numbering of signals as shown in Supplementary Table 8. Black numbers refer to loci reaching the statistical significance threshold in any single-trait analysis, while red numbers refer to loci only reaching statistical significance in the multi-trait analysis.

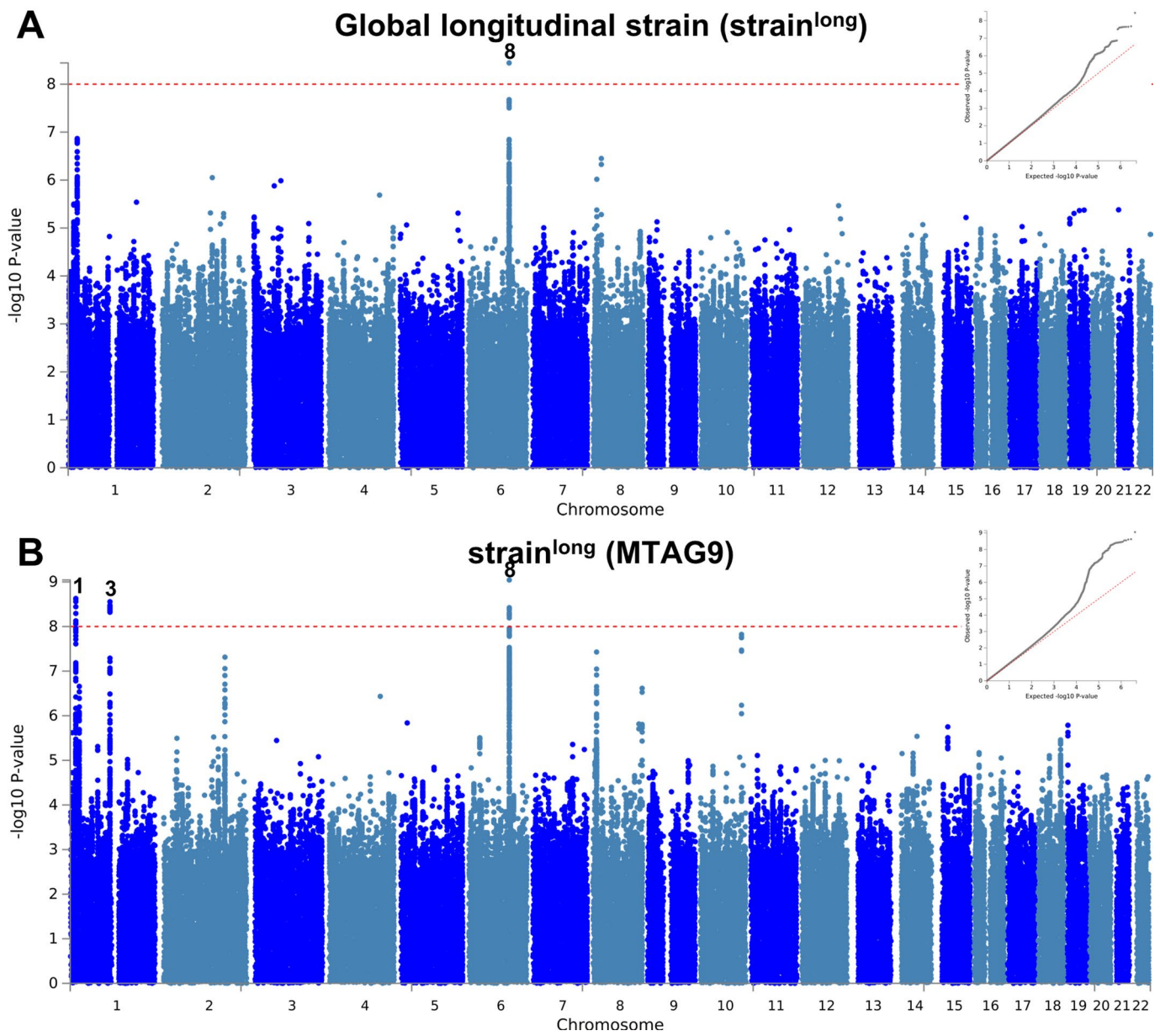

Extended Data Fig. 9 | Manhattan and QQ plots of LV global longitudinal strain GWAS and MTAG. a,**b**, Summary results of the left ventricular global longitudinal strain (strain^{long}) GWAS in the UK Biobank (n=19,260) shown as Manhattan plots for the single-trait (**a**) and the multi-trait analyses (MTAG; **b**). Single-trait analysis (**a**) consisted of a fixed-effects meta-analysis of case–control GWAS using a linear mixed model (BOLT-LMM), and multi-trait analysis results (**b**) were obtained using MTAG including summary statistics for all nine left ventricular (LV) traits. Red dashed line shows the significance threshold of $P=1\times10^{-8}$. Quantile-quantile (QQ) plots shown as inserts in corresponding panels. Genomic inflation (λ)=1.040 (single-trait) and 1.059 (MTAG). Numbering of signals as shown in Supplementary Table 8.

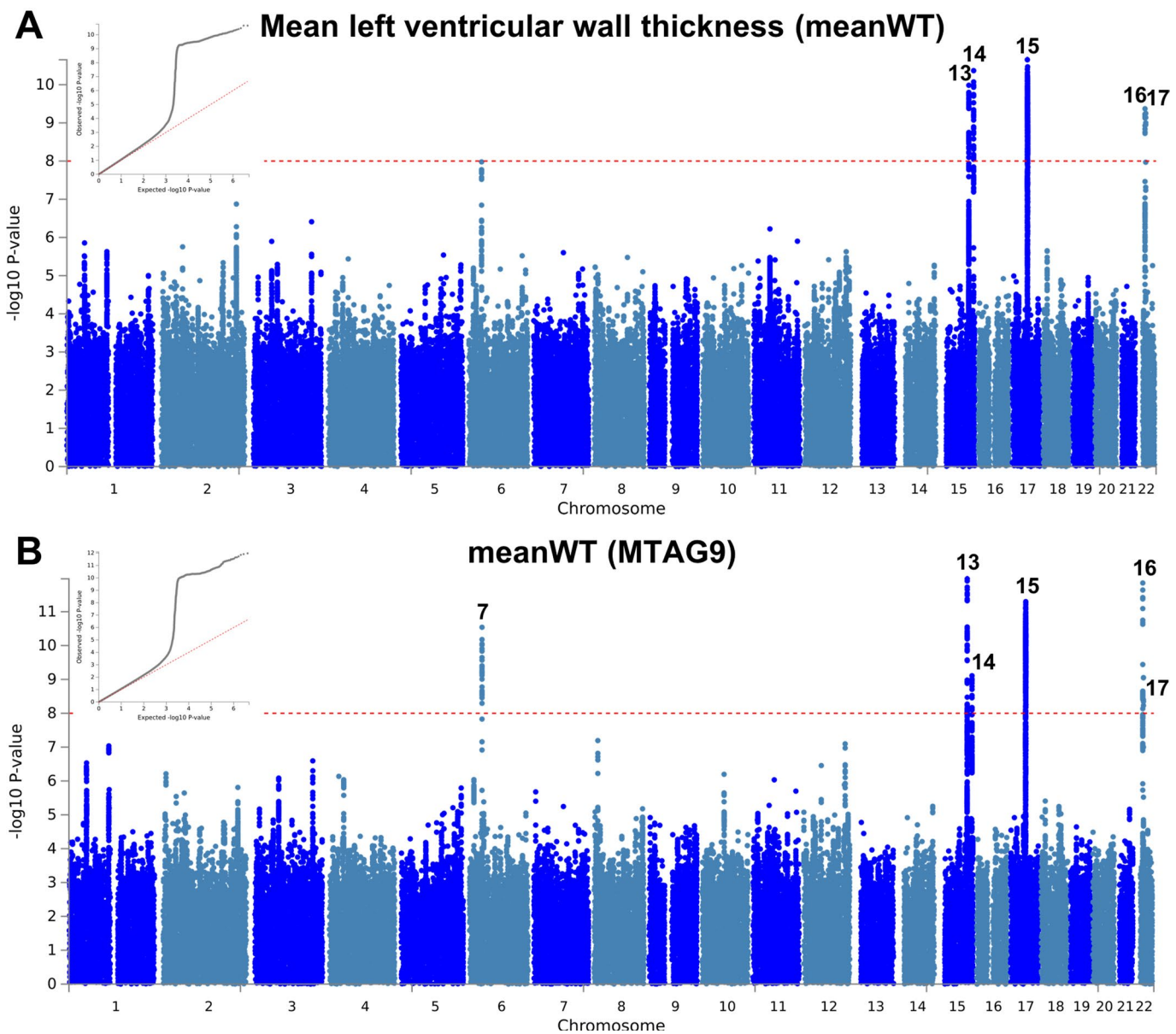

Extended Data Fig. 10 | Manhattan and QQ plots of LV mean wall thickness GWAS and MTAG. a,**b**, Summary results of the mean left ventricular wall thickness (meanWT) GWAS in the UK Biobank (n=19,260) shown as Manhattan plots for the single-trait (**a**) and the multi-trait analyses (MTAG; **b**). Single-trait analysis (**a**) consisted of a fixed-effects meta-analysis of case–control GWAS using a linear mixed model (BOLT-LMM), and multi-trait analysis results (**b**) were obtained using MTAG including summary statistics for all nine left ventricular (LV) traits. Red dashed line shows the significance threshold of $P=1\times10^{-8}$. Quantile-quantile (QQ) plots shown as inserts in corresponding panels. Genomic inflation (λ)=1.065 (single-trait) and 1.072 (MTAG). Numbering of signals as shown in Supplementary Table 8.

nature research

Corresponding author(s): Rafik Tadros, James S Ware, Connie R Bezzina

Last updated by author(s): Sep 6, 2020

Reporting Summary

Nature Research wishes to improve the reproducibility of the work that we publish. This form provides structure for consistency and transparency in reporting. For further information on Nature Research policies, see our Editorial Policies and the Editorial Policy Checklist.

Statistics

For all statistical analyses, confirm that the following items are present in the figure legend, table legend, main text, or Methods section.

n/a	Confirmed
☐	☒ The exact sample size (*n*) for each experimental group/condition, given as a discrete number and unit of measurement
☐	☒ A statement on whether measurements were taken from distinct samples or whether the same sample was measured repeatedly
☐	☒ The statistical test(s) used AND whether they are one- or two-sided *Only common tests should be described solely by name; describe more complex techniques in the Methods section.*
☐	☒ A description of all covariates tested
☐	☒ A description of any assumptions or corrections, such as tests of normality and adjustment for multiple comparisons
☐	☒ A full description of the statistical parameters including central tendency (e.g. means) or other basic estimates (e.g. regression coefficient) AND variation (e.g. standard deviation) or associated estimates of uncertainty (e.g. confidence intervals)
☐	☒ For null hypothesis testing, the test statistic (e.g. *F*, *t*, *r*) with confidence intervals, effect sizes, degrees of freedom and *P* value noted *Give P values as exact values whenever suitable.*
☒	☐ For Bayesian analysis, information on the choice of priors and Markov chain Monte Carlo settings
☒	☐ For hierarchical and complex designs, identification of the appropriate level for tests and full reporting of outcomes
☐	☒ Estimates of effect sizes (e.g. Cohen's *d*, Pearson's *r*), indicating how they were calculated

Our web collection on statistics for biologists contains articles on many of the points above.

Software and code

Policy information about availability of computer code

Data collection	No software was used.
Data analysis	CardioClassifier v0.2.0, PLINK v1.9 and v2.0, Michigan Imputation Server v1.0.2 and v1.2.1, SHAPEIT v2.r790, IMPUTE2 v2.3.2, SNPTEST v2.5.2 and v2.5.4, METAL v2011-03-25, GCTA v1.92.4, R v3.6.0, R package meta v4.9-9, MIRTK toolkit r2.0.0, BOLT-LMM v2.3.2, LDSC v1.0.1, MTAG v1.0.8, R package TwoSampleMR v0.4.25, FUMA v1.3.5, MAGMA v1.07, LDlink v3.9, R package coxme v2.2-14

For manuscripts utilizing custom algorithms or software that are central to the research but not yet described in published literature, software must be made available to editors and reviewers. We strongly encourage code deposition in a community repository (e.g. GitHub). See the Nature Research guidelines for submitting code & software for further information.

Data

Policy information about availability of data

All manuscripts must include a data availability statement. This statement should provide the following information, where applicable:

- Accession codes, unique identifiers, or web links for publicly available datasets
- A list of figures that have associated raw data
- A description of any restrictions on data availability

Data from the Genome Aggregation Database (gnomAD, v2.1) are available at https://gnomad.broadinstitute.org. Data from the UK Biobank participants can be requested from the UK Biobank Access Management System (https://bbams.ndph.ox.ac.uk). Data from the Genotype Tissue Expression (GTEx) consortium are available at the GTEx portal (https://gtexportal.org). Other datasets generated during and/or analyzed during the current study can be made available upon reasonable request to the corresponding authors. Individual level data sharing is subject to restrictions imposed by patient consent and local ethics review boards. Results from meta-analyses of genome-wide association studies reported in this article are available at https://www.heart-institute.nl/gwas and https://data.hpc.imperial.ac.uk [doi.org/10.14469/hpc/7468].

Field-specific reporting

Please select the one below that is the best fit for your research. If you are not sure, read the appropriate sections before making your selection.

☒ Life sciences ☐ Behavioural & social sciences ☐ Ecological, evolutionary & environmental sciences

For a reference copy of the document with all sections, see nature.com/documents/nr-reporting-summary-flat.pdf

Life sciences study design

All studies must disclose on these points even when the disclosure is negative.

Sample size	For hypertrophic cardiomyopathy (HCM), we analyzed the largest sample size available from the Dutch, Royal Brompton and Canadian HCM cohorts, including 1733 unrelated HCM cases and 6628 ancestry-matched controls. For left ventricular (LV) traits, we analyzed the largest sample size with available cardiac magnetic resonance imaging studies from the UK Biobank at the time of analysis, consisting of 19260 individuals. For the study of polygenic risk scores in sarcomeric variant carriers, the largest sample size with available clinical data was used, consisting of 368 carriers of pathogenic or likely pathogenic sarcomeric variants. No method was applied to predetermine sample size.
Data exclusions	HCM case-control GWAS: Samples excluded if genotype missingness rate >0.03, inbreeding coefficient |F|>0.1, sex mismatch, cryptic relatedness up to 3rd degree or are population outliers using genotypic principal component analysis. Following imputation, SNPs were excluded if minor allele frequency (MAF) <0.01, or poor imputation quality (INFO<0.4 for the Royal Brompton stratum, or Minimac R2<0.5 for Dutch and Canadian strata). More stringent quality control was performed for heritability analyses. HCM polygenic risk score (PRS) analyses in sarcomeric variant carriers: PRS was derived from a GWAS excluding sarcomeric variant carriers from the Erasmus Medical Center. We then tested for the association of PRS with disease expression in sarcomeric variant carriers (probands and non-probands) from the Erasmus Medical Center. LV traits GWAS: Exclusion criteria for the UK Biobank imaging substudy included childhood disease, pregnancy and contraindications to MRI scanning. For the LV traits GWAS, we also excluded, by ICD-10 code and/or self-reported diagnoses, any subjects with heart failure, cardiomyopathy, a previous myocardial infarction, or structural heart disease. We also excluded those with uncontrolled hypertension (defined by systolic or diastolic blood pressure >180mmHg or >110mmHg, respectively, at time of imaging visit) or with extremes of body mass index (BMI <16 or >40). We restricted our analysis to Caucasians, defined by genotype. After phenotyping, we also excluded subjects with mean wall thickness >13mm in any of the 16 American Heart Association (AHA) left ventricular (LV) segments, and subjects with outlying (>3 SD from mean) LV mass, LV volumes or LV ejection fraction. We excluded samples with outlying heterozygosity or missingness rates, and those with mismatches between the genotypic and recorded sex. We excluded SNPs failing UK Biobank protocols (filtered per batch by Hardy-Weinberg equilibrium and missingness), those with imputation INFO score <0.3 or MAF <0.01, or with missingness >0.1.
Replication	Replication of HCM loci reaching the significance threshold was tested in an independent dataset comprised of 2,694 cases with HCM included from the Hypertrophic Cardiomyopathy Registry (HCMR) or the NIHR Bioresource for Rare Disease (BRRD), and 47,486 controls without HCM included from the UK Biobank or BRRD. All loci reaching P<1e-8 in the multi-trait analysis were successfully replicated.
Randomization	The main study design is a case control genome-wide association study. HCM cases: participants with a clinical diagnosis of hypertrophic cardiomyopathy. Controls: participants free of HCM.
Blinding	Analysts were not blinded because linking the genotype and phenotype data was necessary for quality control and analyses. Blinding was not relevant to our study. The participants from the included studies were sampled by multiple different research centers. The meta-analyses were conducted centrally on summary level results from each study.

Reporting for specific materials, systems and methods

We require information from authors about some types of materials, experimental systems and methods used in many studies. Here, indicate whether each material, system or method listed is relevant to your study. If you are not sure if a list item applies to your research, read the appropriate section before selecting a response.

Materials & experimental systems

n/a	Involved in the study
☒	☐ Antibodies
☒	☐ Eukaryotic cell lines
☒	☐ Palaeontology and archaeology
☒	☐ Animals and other organisms
☐	☒ Human research participants
☒	☐ Clinical data
☒	☐ Dual use research of concern

Methods

n/a	Involved in the study
☒	☐ ChIP-seq
☒	☐ Flow cytometry
☒	☐ MRI-based neuroimaging

Human research participants

Policy information about studies involving human research participants

Population characteristics	Population characteristics are described in Supplementary Tables 1 (HCM GWAS), 6 (LV traits GWAS) and 20 (PRS analyses).
Recruitment	HCM cases were recruited from Amsterdam University Medical Center (location AMC, Netherlands), University Medical Center Groningen (Netherlands), Erasmus Medical Center (Netherlands), Royal Brompton & Harefield Hospitals (United Kingdom), Montreal Heart Institute (Canada) and London Health Sciences Center (Canada). The LV trait GWAS was performed in participants of the UK Biobank.
Ethics oversight	All components of the study were approved by ethics review boards at corresponding institutions: -Dutch HCM GWAS: Approved by the Medisch Ethische Toetsingscommissie (METC) of the Amsterdam University Medical Center. -UK HCM GWAS: Healthy volunteers were recruited as part of the Digital Heart Project (approved by Hammersmith & Queen Charlotte's Research Ethics Committee). HCM cases came from the Royal Brompton & Harefield Hospital Biobank (Approved by South Central - Hampshire B Research Ethics Committee). -Canadian HCM GWAS approved by the Research Ethics and New Technology Development Committee of the Montreal Heart Institute. -HCM GWAS replication: HCMR approved by South Central - Oxford A Research Ethics Committee. BRRD approved by East of England - Cambridge South Research Ethics Committee. -UK Biobank approved by the UK Research Ethics Committee. Reported analyses conducted under application 18545.

Note that full information on the approval of the study protocol must also be provided in the manuscript.